Published in final edited form as:
J Mol Biol. 2012 March 2; 416(4): 467–485. doi:10.1016/j.jmb.2011.12.048.

Human tRNA$^{Lys3}_{UUU}$ is Pre-Structured by Natural Modifications for Cognate and Wobble Codon Binding through Keto-EnolTautomerism

Franck A. P. Vendeix[1,*], **Frank V. Murphy IV**[2], **William A. Cantara**[1,5], **Grażyna Leszczyńska**[3], **Estella M. Gustilo**[1,§], **Brian Sproat**[4,§], **Andrzej Malkiewicz**[3], and **Paul F. Agris**[1,5,*]

[1]Department of Molecular and Structural Biochemistry, North Carolina State University, 128 Polk Hall, Raleigh, North Carolina, 27695-7622, USA [2]Northeastern Collaborative Access Team, Building 436, Argonne National Laboratory, Argonne, Illinois 60439, USA [3]Institute of Organic Chemistry, Technical University, Żeromskiego 116, 90-924, Łódź, Poland [4]Integrated DNA Technologies BVBA, Provisorium 2, Minderbroedersstraat 17-19, B-3000 Leuven, Belgium [5]The RNA Institute, University at Albany-SUNY, Albany N.Y. 12222 USA

Abstract

Human tRNA$^{Lys3}_{UUU}$ (htRNA$^{Lys3}_{UUU}$) decodes the lysine codons AAA and AAG during translation, and also plays a crucial role as the primer for HIV-1 reverse transcription. The post-transcriptional modifications 5-methoxycarbonylmethyl-2-thiouridine (mcm^{5}s^{2}U$_{34}$), 2-methylthio-N^6-threonylcarbamoyladenosine (ms^{2}t^{6}A$_{37}$)and pseudouridine (ψ_{39}) in the tRNA'santicodon loop are critical for ribosomal binding and HIV-1 reverse transcription. To understand the importance of modified nucleoside contributions, the structure and function of this tRNA's anticodon stem and loop domain were determined with these modifications at positions 34, 37 and 39, respectively (hASL$^{Lys3}_{UUU}$-mcm^{5}s^{2}U$_{37}$;ms^{2}t^{6}A$_{37}$;ψ_{39}). Ribosome binding assays *in vitro*revealed that the hASL$^{Lys3}_{UUU}$-mcm^{5}s^{2}U$_{34}$;ms^{2}t^{6}A$_{37}$;ψ_{39}bound AAA and AAG codons, whereas binding of the unmodified ASL$^{Lys3}_{UUU}$ was barely detectable. The UV hyperchromicity, the circular dichroism and the structural analyses indicated that ψ_{39} enhanced the thermodynamic stability of the ASL through base stacking while ms^{2}t^{6}A$_{37}$ restrained the anticodon to adopt an open loop conformation that is required for ribosomal binding. The NMR-restrained molecular dynamics derived solution structure revealed that the modifications provided an open, ordered loop for codon binding. The crystal structures of the hASL$^{Lys3}_{UUU}$-mcm^{5}s^{2}U$_{34}$;ms^{2}t^{6}A$_{37}$;ψ_{39} bound to the

*Corresponding authors and their current addresses: Paul F. Agris; The RNA Institute, Biological Sciences, University at Albany-SUNY, 1400 Washington Ave, Albany, NY 12222, USA; Phone: 1-518-437-4448; PAgris@albany.edu. FAX: 1-518-437-4456.
*Franck A. P. Vendeix; Sirga Advanced Biopharma, Inc., 2 Davis Drive; P.O. Box 13169; Research Triangle Park, North Carolina, 27709, USA; Phone: 1-919-354-1008;; E-mail: fvendeix@sirgaab.com, FAX: 1-919-990-8561.
§Present addresses: E.M.Gustilo: The Scripps Research Institute, MB-35, 10550 North Torrey Pines Road, La Jolla, CA 92037 USA; estellag@scripps.edu
§B.Sproat: Chemconsilium GCV, Jaarmarktstraat 48, 2221, Booischot, Belgium; fa205401@skynet.be

Accession Numbers The coordinates of X-ray and NMR structures including factors and NMR restraints have been deposited in the Protein Data Bank (RCSB) and the BioMagResBank (BMRB). The accession numbers 2L9E (17449) have been assigned to solution structure of the doubly modified ASL$^{Lys3}_{UUU}$, and the accession numbers 3T1H and 3T1Y were assigned to the crystal structures bound to AAA and AAG, respectively. A complete listing of resolution and structure factors can be accessed in the Protein Data Bank.

Supplementary Data. Supplementary data associated with this article can be found, in the online version.

30S ribosomal subunit with each codon in the A site showed that the modified nucleotides $mcm^5s^2U_{34}$ and $ms^2t^6A_{37}$ participate in the stability of the anticodon/codon interaction. Importantly, the $mcm^5s^2U_{34}$•G_3 wobble base pair is in the Watson-Crick geometry, requiring unusual hydrogen bonding to G in which $mcm^5s^2U_{34}$ must shift from the keto to enol form. The results unambiguously demonstrate that modifications pre-structurethe anticodonas a key prerequisite for efficient and accurate recognition of cognate and wobble codons.

Keywords

Modifications; wobble decoding; anticodon structure; $tRNA^{Lys3}$

INTRODUCTION

Accurate ribosome-mediated protein synthesis requires proper recognition of mRNA codons by specific aminoacylatedtRNAisoacceptors. The influence of post-transcriptional tRNA modifications on translational fidelity has been widely investigated.[1–4] As a result of such studies, 93 different, naturally-occurring modification chemistries have been identified in tRNAs.[5] These modifications, particularly in the anticodon stem and loop domain (ASL), have been shown to significantly impact ribosome binding affinity,[6–8] codon discrimination, thermodynamic stability,[11] speed of translation,[12] recognition by cognate aminoacyl-tRNAsynthetases[13] and reading frame maintenance.[14–17] Specifically, modifications to the wobble nucleoside at position-34 and the conserved purine residue at position-37, 3'-adjacent to the anticodon, are essential for pre-structuring the ASL, permitting proper anticodon conformation and efficient codon recognition. Human $tRNA^{Lys3}_{UUU}$ ($htRNA^{Lys3}_{UUU}$; Fig. 1a,b) is of particular interest because of its dual role in promoting proper endogenous translation and acting as the primer selected for initiation of reverse transcription (RT) by human immunodeficiency virus 1 (HIV-1) and other lentiviruses.[19] Indeed, the ASL modifications present in $htRNA^{Lys3}_{UUU}$ have been shown to be required for efficient initiation of RT in HIV-1.[20–22]

The anticodon stem and loop (ASL^{Lys}_{UUU}) domain of the sole *E. coli* $tRNA^{Lys}_{UUU}$has been studied extensively as a model due to its modified nucleotides being similar to those of the human $tRNA^{Lys3}_{UUU}$ and its anticodon loop nucleoside sequence being identical.[23] The ASL loop modifications of the *E. coli*$tRNA^{Lys}_{UUU}$, 5-methylaminomethyl-2-thiouridine ($mnm^5s^2U_{34}$) and N^6-threonylcarbamoyladenosine (t^6A_{37}), pre-structure the loop into the canonical U-turn conformation that is necessary for efficient binding to synonymous codons in the ribosomal A-site. Both studies *in vitro*[27–29] and *in vivo*[30] have shown that a 2-thiolation, and not 5-methylaminomethylation, at the wobble position acts as a strong positive identity element for recognition of $tRNA^{Lys}_{UUU}$ and $tRNA^{Glu}_{UUC}$ by their respective cognate aminoacyl-tRNAsynthetases. X-ray crystallography of the ASL domain of *E. coli*$tRNA^{Lys}$ on the 30S ribosomal subunit demonstrated clearly that the t^6A_{37} modification further stabilizes the unusually low enthalpy of binding in the A–U rich codon-anticodon interaction by forming a cross-strand stack with the first adenosine residue of the codon.[25] The t^6A_{37} modification and its derivatives are found in the tRNAisoacceptors that decode codons beginning with A in all three Domains of life.

$htRNA^{Lys3}_{UUU}$is one of three lysine isoacceptors found in mammalian species and is responsible for decoding the minor lysine codon AAA, as well as the major AAG codon.[32] The ASL domain of $htRNA^{Lys3}_{UUU}$ is more extensively modified than that of the *E. coli*$tRNA^{Lys}_{UUU}$. The anticodon loop of $hASL^{Lys3}_{UUU}$ has a 5-methoxycarbonylmethyl-2-thiouridine at position-34 ($mcm^5s^2U_{34}$)and a 2-methylthio-N^6-threonyl-carbamoyladenosine at position-37 ($ms^2t^6A_{37}$).[35]Apseudouridineis present at position-39 (ψ_{39}) in the ASL stem,

immediately adjacent to the loop (Fig. 1a,b). In contrast to the htRNA$^{Lys3}_{UUU}$, the ASLs of the isoaccepting htRNA^{Lys1,2}contain an unmodified C_{34} and a more simply modified A_{37} (t^6A_{37}). The htRNA^{Lys1,2}isoacceptors represent two-thirds of all lysine tRNA in mammalian cells, and are specific for decoding only the dominant AAG codon.*In vitro* ribosome binding studies using the hASL$^{Lys3}_{UUU}$ with the *E. coli* modifications, mnm^5U_{34} and t^6A_{37}, demonstrated that the insertion of the individual modifications in the ASL at positions 34 or 37 respectively, would rescue codon binding to only the cognate AAA.With both modifications present the ASL recognized both AAA and AAG.[8] This highlights the importance of the two-hypermodificationsbeing present for dual codon recognition and specificity.

The importance of the hypermodified nucleotides $mcm^5s^2U_{34}$ and $ms^2t^6A_{37}$to thestructure and functions of htRNA$^{Lys3}_{UUU}$have been modeled and some empirical data reported.[8,21,39–41]However, tangible structural evidence of their functional contributions to the fully modified hASL$^{Lys3}_{UUU}$ is still lacking. Here, using NMR, X-ray crystallography and otherbiophysical and biochemical methods, we report the key structure/function relationship for these naturally occurring modifications to the anticodon domain of htRNA$^{Lys3}_{UUU}$. To the best of our knowledge, the modified nucle otides $mcm^5s^2U_{34}$, $ms^2t^6A_{37}$ and ψ_{39} were introduced simultaneously into the hASL$^{Lys3}_{UUU}$ sequence for the first time through chemical synthesis. Codon binding characteristics and atomic resolution structures, both in solution and on the 30S ribosomal subunit, of the doubly modified hASL$^{Lys3}_{UUU}$-$mcm^5s^2U_{34}$,$ms^2t^6A_{37}$ and triply modified hASL$^{Lys3}_{UUU}$-$mcm^5s^2U_{34}$;$ms^2t^6A_{37}$;ψ_{39} show that the modifications are instrumental in the pre-structuring of the loop into an open loop conformation and facilitating keto-enoltautomerismthat is essential for cognate and wobble codon binding.

RESULTS

Recognition of lysine codons at the ribosomal A-site

The triply modified hASL$^{Lys3}_{UUU}$-$mcm^5s^2U_{34}$;$ms^2t^6A_{37}$;ψ_{39} was chemically synthesized in order to determine the effect of the native modifications on its structure and function in binding the cognate and wobble codons AAA and AAG. The site-selected introduction of the complex modifications $mcm^5s^2U_{34}$ and $ms^2t^6A_{37}$ is problematic and required a novel chemical synthesis of the oligonucleotide in which the modified nucleoside functional groups as well as the major bases were transiently protected. The protecting chemistries had to be compatible with each other and with that of the major nucleosides such that all are readily and quantitatively removed when the oligonucleotide synthesis was complete. The cyclic chemistry involves the repeated coupling of a nucleoside phosphoramiditeto the growing sequence and, at each addition, the oxidation of the trivalent phosphate into a pentavalent phosphate. Removal of the oligonucleotide from the solid support and deprotection of the C2'-OH are accomplished under conditions that would normally alter the modified nucleosides. A novel use of protecting agents and an alteration of the deprotection protocol maintained the native integrity of the modifications (Supplementary Fig. S1). The presence of the modifications in stoichiometric amounts was quantified by nucleoside composition analysis with HPLC (Supplementary Fig. S2), and observed in NMR and X-ray crystallography. The terminal base pair ψ_{27}•A_{43} was substituted with a G_{27}•C_{43} pair to enhance stability of the ASL constructs (Fig. 1a).

The triply modified hASL$^{Lys3}_{UUU}$-$mcm^5s^2U_{34}$;$ms^2t^6A_{37}$;ψ_{39} bound AAA and AAG at the A-site of the *E. coli* ribosome with a high affinity, dissociation constants (K_d) of 3.1 ± 0.4 μM and 3.9 ± 0.8 μM, respectively (Fig. 2a,b). In contrast, the unmodified ASL$^{Lys3}_{UUU}$ exhibited very poor binding to both lysine codons. The equilibrium binding of the unmodified hASL$^{Lys3}_{UUU}$ to either of the lysine codons AAA or AAG was nearly

undetectable (Fig. 2a,b). Previously, we had observed that the single atom substitution of sulfur for oxygen at the 2-position of U_{34} rescued ASL^{Lys}_{UUU} binding of the cognate and wobble codons, and that the introduction of only t^6A_{37} enabled AAA binding, but not AAG binding or translocation to the P-site.[6,8,15,25,42] Our experiments with the unmodified and modified $hASL^{Lys3}_{UUU}$-$mcm^5s^2U_{34}$;$ms^2t^6A_{37}$;ψ_{39} revealed that anticodon domain modifications enhanced codon binding, similar to results reported for the variously modified anticodon domain of the bacterial $tRNA^{Lys}_{UUU}$ (ASL^{Lys}_{UUU}-s^2U_{34}, ASL^{Lys}_{UUU}-mnm^5U_{34}, ASL^{Lys}_{UUU}-t^6A_{37} and ASL^{Lys}_{UUU}-mnm^5U_{34};t^6A_{37}).[7,8]

Anticodon loop modifications alter thermal stability

A comparison of the thermal stabilities of the differently modified $hASL^{Lys3}_{UUU}$ constructs by UV-monitored thermal denaturation revealed both similarities and distinct differences in their thermodynamic properties. While the enthalpy (ΔH), entropy (ΔS) and standard free energy (ΔG) did not vary significantly, the introduction of modifications caused a reduction in the melt temperature, T_m, at which half of the RNA molecules are denatured.The $hASL^{Lys3}_{UUU}$-$mcm^5s^2U_{34}$;$ms^2t^6A_{37}$ and the $hASL^{Lys3}_{UUU}$-$mcm^5s^2U_{34}$;$ms^2t^6A_{37}$;ψ_{39}exhibited a T_m of ~53 °C in comparison toa T_m of ~57 °C for the unmodified $hASL^{Lys3}_{UUU}$ (Fig. 2c, and Table 1). Even so, the $hASL^{Lys3}_{UUU}$-$mcm^5s^2U_{34}$;$ms^2t^6A_{37}$;ψ_{39}exhibited the greatest degree of hyperchromicityin comparison to the unmodified $hASL^{Lys3}_{UUU}$ and the $hASL^{Lys3}_{UUU}$-$mcm^5s^2U_{34}$;$ms^2t^6A_{37}$; (Fig. 2c and Table 1). The degree of hyperchromicity is a measure of base stacking and overall molecular order.

Modifications may affect the molecular order of the anticodon through base stacking interactions. Relative base stacking interactions are readily observed by comparison of circular dichroism spectra. The circular dichroism(CD) spectra of the ASLs were analyzed at the maximum positive ellipticityof 264 nm. A negative ellipticity at a wavelength of λ = 330 nm and positive ellipticity at λ = 310 nm for both the doubly and triply modified ASLs was also observed (Fig. 2d). These ellipticities are in agreement with characteristics typical of a 2-thio modified uridine.[43] The $hASL^{Lys3}_{UUU}$-$mcm^5s^2U_{34}$;$ms^2t^6A_{37}$;ψ_{39} exhibited a small but reproducibly greater positive ellipticityat 264 nm than the other two ASLs, suggesting again a higher degree of order.

Structure of the ASL^{Lys3}_{UUU}-$mcm^5s^2U_{34}$;$ms^2t^6A_{37}$in solution

Sequence-specific NMR resonance assignments—The results of the UV-monitored thermal denaturations and CD spectroscopy implied that the $mcm^5s^2U_{34}$, $ms^2t^6A_{37}$ and ψ_{39} modifications may play a role in ordering the dynamic structure of the $hASL^{Lys3}_{UUU}$. To study and understand the extent to which these modifications affect the anticodon conformation and dynamics, the three dimensional (3D) solution structure of the doubly modified $hASL^{Lys3}_{UUU}$-$mcm^5s^2U_{34}$;$ms^2t^6A_{37}$ was determined through NMR and restrained molecular dynamics. In addition, the structure of its unmodified counterpart was fully characterized by NMR. In achieving this goal, the identification and sequence-specific assignment of the nucleotide spin systems was completed by using combinations of homo-(^{1}H-^{1}H)-nuclear and natural abundance hetero-(^{1}H-^{13}C; ^{1}H-^{31}P)-nuclear 1D and 2D NMR experiments conducted in H_2O or D_2O solvent.Well-established protocols were employed for the assignment of nucleic acid resonances in the absence of isotopic labeling.[44,45] The NMR spectra were recorded in the absence of Mg^{2+} because previous experiences revealed that the addition of a physiological amount of Mg^{2+} ions (1–5 mM) to the modified ASL samples did not significantly affect the resulting NMR spectra. The addition of larger concentrations of Mg^{2+} induced spectral line broadening in some ASLs.[11,46,47]

Exchangeable protons—The imino and amino protons of the doubly modified hASL$^{Lys3}_{UUU}$-mcm^{5}s^{2}U$_{34}$;ms^{2}t^{6}A$_{37}$ were identified and assigned using ^{1}H 1D and ^{1}H-^{1}H 2D NOESY NMR spectra that were recorded in H_2O at 2 °C.In assigning the exchangeable protons,we used the initial assumption that the stem of the ASL was reasonably close to A-type RNA conformation, as was indicated by CD spectroscopy (Fig. 2d). Four resonance signals were observed in the low field region (12.50 – 14.00 ppm) of the ^{1}H 1D spectrum of the hASL$^{Lys3}_{UUU}$-mcm^{5}s^{2}U$_{34}$;ms^{2}t^{6}A$_{37}$. These NMR signals were characteristic of imino protons that are engaged in Watson-Crick base pairs and were sequentially assigned to the G$_{27}$H1, G$_{42}$H1, U$_{41}$H3 and G$_{30}$H1 (Supplementary Fig. S3). The resonance peak of the G$_{27}$H1 displayed a low intensity and broad line width which is expected from the terminal base pair G$_{27}$•C$_{43}$. The resonance signal corresponding to the H1 imino proton of U$_{39}$ that is engaged in the A$_{31}$•U$_{39}$ base pair adjacent to the loop could not be identified. Therefore, this imino proton was not assigned. The assignment of the imino protons allowed us to fully assign the amino protons of the nucleotides of the stem. Under our NMR experimental conditions (see Methods and Materials) the rapidly exchanging amino and imino protons of the loop nucleosides could not be identified.

Interestingly, the HN proton of the amide group of the threonyl moiety of ms^{2}t^{6}A$_{37}$ (Fig. 1b) was clearly identified due to the distinctive chemical shift of its resonance peak observed at 9.66 ppm (Fig. 3). Nuclear Overhauser effect (NOE) cross-peaks were observed between HN and s^2-CH$_3$, between HN and Hβ of the methylene group and between HN and the gamma methyl group, CγH_3, of the threonylmoiety (Fig. 3). However, a very weak NOE connectivity between HN and Ha was hardly visible at 2 °C. Additionally, at 2 and 22 °C, NOE signals between the water molecules and the assigned imino and amino protons were observed, except in the case of HN. Also an NOE was detected between CγH_3 and s^2-CH$_3$.

Non-exchangeable protons—The H6 and H5 aromatic protons of the nine unmodified pyrimidines of the doubly modified hASL$^{Lys3}_{UUU}$-mcm^{5}s^{2}U$_{34}$;ms^{2}t^{6}A$_{37}$ could readily be identified as a result of the presence of intense cross-peaks observed in the COSY and TOCSY spectra (between F_1 = 5.18 – 5.90 ppm and F_2 = 7.30 – 7.90 ppm). The cross-peaks of the cytidines and uridines were differentiated from each other by using their respective ^{13}C chemical shifts detected in the ^{1}H-^{13}C HSQC spectrum. The H6 proton of the modified uridinemcm^{5}s^{2}U$_{34}$ was identified on the ^{1}H-^{13}C HSQC and later assigned on the NOESY spectra. Sequential assignments were obtained within the aromatic to H1' resonance region of the NOESY spectra (F_1 = 5.18 – 6.60 ppm and F_2 = 6.90 – 8.40 ppm). An NOE walk (Supplementary Fig. S4), that is characteristic of A-form RNA conformation, could be observed through intra/inter-nucleotide NOE cross peaks occurring from G$_{27}$H1'-H8 to G$_{43}$H1'-H6. Disruptions in the NOE walk only occurred in the anticodon loop between mcm^{5}s^{2}U$_{34}$ H1'-H6 and mcm^{5}s^{2}U$_{34}$ H1'-U$_{35}$H6 and between ms^{2}t^{6}A$_{37}$ H1'-H8 and ms^{2}t^{6}A$_{37}$H1'-A$_{38}$H8.

The relatively small size of the heptadecamerASL, and the high level of purity of the NMR samples combined with the good resolution and dispersion of the NMR cross-peaks allowed us to achieve a near-complete assignment of the non-exchangeable proton resonances. The H5′/H5” protons were not entirely identified and assigned as a result of spectral overlap. Despite the disruptions in the NOE walks, NOE connectivities that were important for structure determination were observed between the unmodified and modified nucleotides of the loop region (Supplementary Fig. S4).

Modifications may affect the presence of a canonical U-turn in the anticodon loop at the invariant U$_{33}$. Therefore, the solution structure of the doubly modified ASL was investigated for proton and phosphorus resonances that characterize the U-turn. The canonical U-turn conformation in RNAs is confirmed through a distinctive ^{1}H-NMR “fingerprint.”[48] This

fingerprint usually consists of NOE signalsbetween the anomeric H1' proton of the conserved U_{33} and its own H5/H6, and between the anomeric H1' proton of U_{33} and the U_{35}H5/H6. In addition, U_{33}H2' has NOE connectivities to H5/H6 of bases U_{34} and U_{35}. Also, the phosphorus of the dinucleotide $U_{33}33pU_{34}$ has a strong down-field chemical shift which reflects the fact that the a dihedral angle is *trans*. In our study, an NOE was observed between U_{33}H1' and its own aromatic protons for the doubly modified hASL$^{Lys3}_{UUU}$-mcm^{5}s^{2}U$_{34}$;ms^{2}t^{6}A$_{37}$. Another NOE connectivity was detected between U_{33}H2' and mcm^{5}s^{2}U$_{34}$H6. Interestingly, CγH3 of the methylene group of mcm^{5}s^{2}U$_{34}$ gave a medium strength NOE signal to U_{33}H1'. The ^{1}H-^{31}P HETCOR NMR experiment showed that the chemical shifts of the resonances for the ^{31}P nucleus were narrowly confined (Supplementary Fig. S5), as commonly observed in the case of A-RNA.[44,49]

Solution structure of the hASL$^{Lys3}_{UUU}$-mcm^{5}s^{2}U$_{34}$;ms^{2}t^{6}A$_{37}$—The distance and angle restraints required for the structure calculation were determined following the NMR spectral analyses.[44] A total of 552 NOE-derived distance restraints were used for the structure calculation. These distance restraints were constituted by 392 and 134 NOE distance restraints that were assigned to the stem and the loop, respectively. In addition, 26 hydrogen bond (hb) and five planarity restraints were also used to define the structure of the stem. A total of 126 dihedral angle restraints were also used to determine the entire structure of the ASL. The results of the UV thermal denaturation, the CD experiments and the pattern of the anomeric-aromatic NOE walk strongly suggested that the stem of the doubly modified ASL adopted an A-RNA conformation. Therefore, the NMR torsion-angle and distance restraints from the stem were complemented with distance restraints that yield the conventional A-form helix RNA conformation, as previously described and employed by others.[47,48]

The ten lowest energy structures determined from the torsion angle molecular dynamics calculations that were in agreement with the NMR data were selected to represent the final ensemble (Fig. 4). The final set of solution structures was chosen on the basis of displaying not a single NOE restraint violation superior to 0.5 Å and no dihedral angle violations greater than 5°. In addition to these selection criteria, structures were rejected if their root-mean square deviations (rmsds) of bonds and angles varied from ideal values, i.e. by greater than 0.02 Å and 2.0°, respectively. The pairwise rmsd for all atoms is 0.82 ± 0.20 Å.

As expected, the stem of the ASL$^{Lys3}_{UUU}$-mcm^{5}s^{2}U$_{34}$;ms^{2}t^{6}A$_{37}$ exhibited typical features characteristic of A-RNA conformation with Watson-Crick base pairs[50] (Supplementary Fig. S6). The unmodified nucleotides of the stem adopted an anti-parallel geometry with a glycosyl C1'-C1' distance of ~10.6 Å. The sugar moieties adopted the C3'-*endo* conformation except those of residues U_{33} and mcm^{5}s^{2}U$_{34}$ showing C4'-*exo* and C2'-*exo* puckers, respectively. The nucleotides of the loop appeared to be stacked. The distance between the horizontal planes of ms^{2}t^{6}A$_{37}$ and U_{36} was wider by 2 Å in comparison to that between ms^{2}t^{6}A$_{37}$ and A_{38}. Residues 33–37 of the loop displayed local base step parameters (tilt and roll) that deviated from the standards of A-form helices, but resulted in a stacked anticodon. As a result the labile proton of the acid group of ms^{2}t^{6}A$_{37}$ is in close proximity (2.8 Å) to U_{34} and U_{35}O4. The distance between A_{38}N6 and C_{32}O2 proximal to the stem was determined to be 3.5 Å, thereby invoking the potential of hydrogen bonding and the limited extension of the stem (Supplementary Fig. S6).

Crystal structures of the hASL$^{Lys3}_{UUU}$interaction with mRNA on the ribosomal 30S subunit

The crystal structures of the triply modified hASL$^{Lys3}_{UUU}$-mcm^{5}s^{2}U$_{34}$;ms^{2}t^{6}A$_{37}$;ψ_{39} bound to the cognate 5'-AAA-3' and wobble 5'-AAG-3' codons were obtained by soaking native *Thermusthermophilus* 30S ribosomal subunit (30S) crystals with the relevant RNA

oligonucleotides. The A-site binding antibiotic paromomycin was included to improve both the resolution of the data and the occupancy of the ASL. This has been shown not to change the structure of the codon-anticodon complex itself.[51] The recognition of the cognate codonanticodon complex in the 30S decoding center is identical to structures reported previously.[51] As already observed for other cognate recognition structures,[25,52] the structure of the 30S itself is identical within experimental error compared to its published structures. This invariance of the 30S allows the differences in ASL structures to be unambiguously attributed to the modifications of the ASL alone.Additionally, the high resolution of the structures, 3.1 Å and 2.8 Å for AAA and AAG respectively (Supplementary Table S1), allowed for unambiguous determination of the geometry of the ASL and the codon-anticodon interaction.

Contributions of $ms^2t^6A_{37}$ and $mcm^5s^2U_{34}$ to $tRNA^{Lys3}_{UUU}$ and codons recognition—The N^6-threonylcarbamoyl (t^6) modification of A_{37} functions in codon binding, using three different mechanisms as observed previously.[25] First, the t^6 modification abrogates the possible U_{33}•A_{37} base pair, in effect pre-ordering the $hASL^{Lys3}_{UUU}$ in a conformation for codon recognition.[53] This open loop conformation of the anticodon seems to be critical for codon binding, at least for the case of the UUU anticodon.[8] Additionally, the ureido group of the t^6 modification forms a pseudo-heterocycle stabilized by a hydrogen bond from N to N1 of the modified adenine base and by the significant charge delocalization within the group. This planar structure is used to increase stacking of the $ms^2t^6A_{37}$ with A_{38}, its 3' neighbor (Fig. 5a). Finally, the threonyl moiety is too bulky to be incorporated into the helical stack (Supplementary Fig. S7), so it serves to sterically position the pseudo-three cycle base in a very specific location in order to make a cross-strand stack which bridges from the ASL's 3' stack to the codon itself. This cross-strand stack greatly enhances the stability of the codon-anticodon complex.

The 2-methylthio (ms^2) modification of A_{37} functions to enhance the stacking interactions with A1 of the codon, as predicted by a fortuitous crystal packing interaction in the crystal structure of the tRNA alone.[54] The sulfur of the ms^2 modification is positioned to stack proximally to the ring of the codon base A1. It has been shown that placement of a stacking sulfur such that it can interact with an N1 of the stacking partner maximizes the strength of the interaction,[55] and in the current case, it also stacks well with an S_2-N characteristic, albeit with the N7 rather than the N1 of the codon base A1 (Fig. 5b). This provides strong evidence that the sulfur of the ms^2 modification acts primarily to enhance the stacking of $ms^2t^6A_{37}$ with the first base of the codon. The two modifications act in concert to optimize the structure of the anticodon loop in an open conformation prior to codon binding, and to maximize the strength of the codon-anticodon interaction by forming a sulfur-enhanced cross-strand stack by the precisely-positioned pseudo-three cycle base. In the absence of the ms^2, the t^6 takes the same position in the 3'-stack of the ASL as it does in its presence. This conserved positioning of the t^6 is clearly seen in a superimposition of the crystal of what would be the bacterial ASL^{Lys}_{UUU}-t^6A_{37} and ASL^{Lys}_{UUU}-mnm^5U_{34};t^6A_{37}[25] with that of the $hASL^{Lys3}_{UUU}$-$mcm^5s^2U_{34}$;$ms^2t^6A_{37}$;ψ_{39} (Fig. 5c).

Although this is the first structure of the base $mcm^5s^2U_{34}$ bound to its cognate and wobble codon bases A and G, respectively, there are studies that have provided important evidence as to how the modifications function. It has been shown that the 5-methoxycarbonylmethyl (mcm^5) modification promotes the binding of G-ending codons, but not A-ending codons. In contrast, the 2-thio (s^2) modification has been shown to promote binding to both codons,[39] but particularly to A.[7,56]The s^2, and not the 5-position modification, produces the significantly more stable, *anti* C3'-*endo*, g^+ conformation, and transfers a similar restraint to the 3'-neighbor.[57]In studies of ASLs, it has been demonstrated that mcm^5U_{34} has little measurable effect on structure, but that s^2U_{34} increases the amount of stacking between U_{34}

and U_{35}.[41] This is evident when comparing the anticodon structure of the A-site hASL$^{Lys3}_{UUU}$-mnm^{5}U$_{34}$;t^{6}A$_{37}$ with that of the hASL$^{Lys3}_{UUU}$-mcm^{5}s^{2}U$_{34}$,ms^{2}t^{6}A$_{37}$ψ$_{39}$ (Fig. 6). The mcm^{5}s^{2}U$_{34}$ is more strongly stacked with s^2 on the nucleobase of U_{35} than is the mnm^{5}U$_{34}$. In fact, s^2 was shown to stack directly on the aromatic ring of U_{35} in a crystal structure of the tRNA alone.[54] The s^2 modification is used to maximize stacking interactions with U_{35} (Fig. 6), stacking close to N1 of the ring, the optimal position for maximal stacking interactions.[55] The current crystal structures explain all of these observations and offer an integrated explanation for the functioning of these two modifications.

The structure of the mcm^{5}s^{2}U$_{34}$•A$_3$ base pair is in the conventional Watson-Crick geometry, as expected (Fig. 7a). The mcm^5 modification does not appear to play a significant role in decoding AAA. However, the s^2 modification is unambiguously participating in a stacking interaction with U_{35}, as anticipated from the tRNA crystal structure. This rationalizes the results for binding to A in previous studies,[6,7,38,56,58] where a position 34 modification was shown to display a higher binding affinity to A but not G; whereas, s^2 enhanced the binding affinity to both A and G.

The structure of the mcm^{5}s^{2}U$_{34}$•G3 base pair is again in the Watson-Crick geometry, but this is more unusual because to pair with G3 through hydrogen bonding in this geometry, mcm^{5}s^{2}U$_{34}$ must shift from its keto to an enol form (Fig. 7b). The keto to enoltautomerism has been observed in the case of uridine 5-oxyacetic acid, cmo^{5}U, in tRNA^{Val}, binding to G.[52]Therefore, it is not surprising for this base pair configuration to occur for mcm^{5}s^{2}U. However, atautomerismof mnm^{5}U$_{34}$ has not been observed in its binding of G3.[25] The geometries of the mcm^{5}s^{2}U$_{34}$ and mnm^{5}U$_{34}$ base paring to G3 are significantly different with the size of the s^2-group a contributing factor to the positioning of the thiolated base (Fig. 7c). Whereas the thiol positions the mcm^{5}s^{2}U$_{34}$, the main function of the mcm^5 modification is to modify the electronic structure of the ring. This shift of the keto-enol equilibrium far enough towards enol enables hydrogen bonding of the mcm^{5}s^{2}U$_{34}$•G3 base pair.

DISCUSSION

Modifications structure and thermodynamically restrain the anticodon loop

The pre-structured and constrained tRNA anticodon is energetically advantageous for a cell's protein synthesis. Every anticodon (other than that of initiator tRNA) must conform to the constraints of the ribosome's A-site, and yet present a physicochemical face that repeatedly reads only the appropriate codons. Repeated use of a conformed and dynamically restricted anticodon negates the need for remodeling the RNA each time an aminoacyl-tRNA is used for the decoding of its synonymous codons. Thus, pre-structuring of the anticodon enhances the accuracy and efficiency of protein synthesis. Though this is true of a great many tRNAs, the tRNA$^{Lys}_{UUU}$ species is of particular interest for two reasons. First, approximately half of all bacteria have one lysine tRNAisoacceptor, the tRNA$^{Lys}_{UUU}$ that has a 5-methylaminomethyl-2-thiouridine modification at wobble position 34 and a *N*^{6}-threonylcarbamoyladenosine, which allows it to respond to both lysine codons AAA and AAG.[23] In contrast, mammalian cells contain three lysine isoacceptingtRNA species for cytoplasmic protein synthesis. The mammalian tRNA$^{Lys1}_{CUU}$ and tRNA$^{Lys2}_{CUU}$ constitute the majority of lysine tRNAs in the cell and respond only to AAG, the prominent lysine codon. The tRNA$^{Lys3}_{UUU}$ is the least abundant of the three isoacceptors in the cell and responds to AAA and AAG. Second, the host cell tRNA$^{Lys3}_{UUU}$ is selected by HIV as the primer for the initiation of reverse transcription as predicted from the viral RNA sequence.[59–61]

The individual modificationsof mnm^{5}U$_{34}$ at the wobble position and t^{6}A at position-37 enhanced the cognate codon binding of the unmodified ASL$^{Lys3}_{UUU}$by approximately seven-fold; however, the modifications in combination increased codon binding to a level equivalent to that of endogenous *E. coli*tRNA$^{Lys}_{UUU}$.[8] The combination of t^{6}A$_{37}$ and mnm^{5}U$_{34}$ or s^{2}U$_{34}$ also allowed efficient wobble codon recognition, but the s^2-modification was required for proper translocation to the P-site.[6,8,25,56]The 2-thiolated uridine at the wobble position of many tRNAs, as well as that of htRNA$^{Lys3}_{UUU}$, causes a slight enhancement of ribosome binding to A over G at the third position of the codon.[6,38,58] Molecular dynamics simulations of the xm^{5}s^{2}U mononucleoside bound to A or G also showed a marked preference for binding to A.[62] Previous NMR experiments investigating xm^{5}s^{2}U as a mononucleoside and in short polymers showed a strong steric preference for the modified uridine to adopt an *anti*, C3'-*endo* sugar pucker conformation, effecting the same in 3'-neighboring nucleosides. Thus, the thio-moiety causes a more rigid binding geometry that could account for selection against pyrimidines at the third position of the codon.[57,58,63,64]

Molecular dynamics simulations also confirmed that the ms^{2}t^{6}A$_{37}$ reduced thermal stability via a stereochemical effect that widened the loop and prevented the A$_{37}$•U$_{33}$ cross-loop interaction.[40] In contrast, structural models of the unmodified ASLs of tRNA$^{Lys}_{UUU}$ and those singly modified with ψ$_{39}$ that had been generated using a subset of NMR distance restraints indicated a thermally stable, closed UUU triloop structure.[41] Consistent with previous *in silico* models and empirical studies, the addition of ms^{2}t^{6}A$_{37}$ to models of the singly modified ASL$^{Lys}_{UUU}$-ψ$_{39}$ also enhanced the stacking interaction of A$_{37}$ with U$_{36}$ and created a more defined positioning of U$_{36}$.[41] According to the models, neither the mcm^5- nor s^2-moieties of U$_{34}$ were sufficient to promote a canonical U-turn conformation. However, the singly modified ASL with mcm^{5}s^{2}U$_{34}$ showed many U-turn NMR indicators.[41] These models suggested a role for the ms^{2}t^{6}A$_{37}$ in negating intraloop interactions, ordering of the anticodon loop conformation and stabilizing the weak U$_{36}$•A1 pair while mcm^{5}s^{2}U$_{34}$ enhanced anticodon base stacking and promoted the canonical U-turn conformation.

Empirical and *in silico* structural studies conclude that these modifications enhance codon recognition by acting to remodel the highly constrained and unfavorable conformation of the unmodified ASL toward a more canonical shape.[6,26,41,53,65,66] Although these studies have shown that the modifications push the equilibrium toward a U-turn structure, it has been unclear as to whether the solution conformation of the fully modified ASL would be sufficiently pre-structured to explain the high level of endogenous codon specificity and fidelity. Here we conclusively show that the fully modified solution structure conforms to a structure that shows only minor differences from the stably bound crystal structure in the ribosomal A-site. In fact, our data also supports the notion that the pre-structuring has underlying thermodynamic causes and allows for a novel keto-enol mechanism of exclusively recognizing purines at the third codon position.

The thermodynamic causes of modification-induced pre-structuring are evident in the thermal melting and circular dichroism spectra. The negative 330 nm and positive 330 nm signals observed in the CD spectrum of the modified ASLs were due to the presence of the 2-thio modification of uridine as previously observed,[43] confirming the presence of this modification in the doubly and triply modified ASLs. The slightly higher value of the positive ellipticityat 264 nm found in the case of the hASL$^{Lys3}_{UUU}$-mcm^{5}s^{2}U$_{34}$;ms^{2}t^{6}A$_{37}$;ψ$_{39}$ indicated that the bases were involved in stacking interactions that exceeded those of both the unmodified hASL$^{Lys3}_{UUU}$ and the doubly modified hASL$^{Lys3}_{UUU}$-mcm^{5}s^{2}U$_{34}$;ms^{2}t^{6}A$_{37}$ (Fig. 3d). These results are not surprising as the introduction of mcm^{5}s^{2}U$_{34}$ and ms^{2}t^{6}A$_{37}$ negated intra-loop hydrogen bonding, reducing

the melting temperature and enthalpy of base stacking.Indeed it has been shown that modifications most likely affect codon bias by contributing significantly to the thermodynamic stability and structural characteristics of htRNA$^{Lys3}_{UUU}$. Modifications of the Watson-Crick face of the invariant purine 37 decrease the thermal stability of the ASL by negating intra-loop hydrogen bonds and by widening the loop, as was initially found for the m^{1}G$_{37}$ of yeast tRNA^{Phe}.[11,65,67] The modification of A$_{37}$ to t^{6}A$_{37}$ and to ms^{2}t^{6}A$_{37}$ in an otherwise unmodified anticodon stem and loop domain of htRNA$^{Lys3}_{UUU}$ resulted in decreases in thermal stability of 2–3 and 5 °C, respectively.[53,68]{Bajji, 2002 #465}However, by negating the intra-loop hydrogen bonding, the base stacking at the base of the stem is alleviated, which resulted in only minor differences in ellipticity between the constructs. ψ$_{39}$ is known to stabilize tRNA's anticodon domain,[66,69] but does not appear to effect codon binding.[69]The presence of pseudouridine at position-39 enhanced the interaction with A$_{31}$ that constitutes the closing base pair of the stem[40,41,66] and stabilized the canonical U-turn conformation,[41] thereby raising the thermal stability of the ASL and increasing the base stacking of the anticodon residues.

The variations in ^{1}H NMR chemical shifts observed when comparing the unmodified and the modified ASLs (Supplementary Table S2) suggested that the spatial electronic environments of the aromatic atoms of mcm^{5}s^{2}U$_{34}$, U$_{36}$, A$_{38}$ and U$_{39}$ were affected by the introduction of the modified residues within the ASL. The invariant chemical shifts were mostly seen for the residues of the stem attesting that the presence of mcm^{5}s^{2}U$_{34}$ and ms^{2}t^{6}A$_{37}$ in the loop did not structurally influence the helical A-RNA conformation of the stem. The greater distance observed between ms^{2}t^{6}A$_{37}$ and U$_{36}$ could have been induced by the large atomic radius of the sulfur group trying to accommodate itself between the above residues. The short distances found between the labile proton of the acid group of ms^{2}t^{6}A$_{37}$ and mcm^{5}s^{2}U$_{34}$/U$_{35}$O4 and between A$_{36}$N6 and C$_{32}$O2 invoked the potential hydrogen bonding that restrained the threonyl group of ms^{2}t^{6}A$_{37}$ to be positioned across the loop region. As a result the loop extension was limited. The NOE observed between C$_{10}$H$_3$ and s^2-CH$_3$ indicated the close spatial proximity (4 – 5 Å) of these two groups. As a result, a clear orientation of these methyl groups was obtained during the solution structure determination of the doubly modified ASL$^{Lys3}_{UUU}$. The lack of a complete set of the signature NMR resonances for a U-turn indicated that the loop of the modified hASL$^{Lys3}_{UUU}$ did not have a canonical U-turn, but nonetheless exhibited a backbone turn at U$_{33}$ in the NMR-restrained molecular dynamics derived structure.

Here, we have shown that the extensive post-transcriptional modifications of the htRNA$^{Lys3}_{UUU}$ pre-structure the anticodon domain for codon binding, and alter the chemistry of the wobble position uridine to engage in a Watson-Crick base pair with the G3 of the AAG codon. Previously, we had determined and compared the codon binding properties, NMR-derived solution structures and crystallographic structures of codon binding of the ASL$^{Lys}_{UUU}$ with and without the bacterial modifications, mnm^5- and t^{6}A$_{37}$.[8,53] Now, we can compare the structures of the hASL^{Lys3}-mcm^{5}s^{2}U$_{34}$;ms^{2}t^{6}A$_{37}$;ψ$_{39}$ presented here with a previous structure in solution,[53] and to that of the crystal structure of the entire htRNA$^{Lys3}_{UUU}$.[54]

Comparison of the solution structures

A structural comparison of the solution structure of hASL$^{Lys3}_{UUU}$-mcm^{5}s^{2}U$_{34}$;ms^{2}t^{6}A$_{37}$ to that of the singly modified hASL$^{Lys}_{UUU}$-t^{6}A$_{37}$[53] reveals a significant, modification dependent rearrangement of the loop region (Fig. 8a).However, the nearly superimposable nature of the stems renders the overall rmsd quite low (Supplementary Table S3b).At the base of the stem, the possibility for the classically bifurcated cross-loop hydrogen bond is slightly perturbed from that of the singly modified structure (Fig. 8b). In the doubly modified hASL$^{Lys3}_{UUU}$-mcm^{5}s^{2}U$_{34}$;ms^{2}t^{6}A$_{37}$, the distance between the bases are increased

from 3.0 Å in the singly modified structure to 3.4 Å. The stacking interaction between $ms^2t^6A_{37}$ and A_{38} in $hASL^{Lys3}_{UUU}$-$mcm^5s^2U_{34}$;$ms^2t^6A_{37}$is in a more favorable geometry, presumably stabilizing A_{38} into a less favorable cross-loop interaction, resulting in a more open and more canonical loop structure (Fig. 8b).

Although the anticodon of doubly modified $hASL^{Lys3}_{UUU}$-$mcm^5s^2U_{34}$;$ms^2t^6A_{37}$ in solution did not contain a canonical U-turn conformation, the hypermodified nucleosides shift the structure into a structure that is more indicative of a U-turn than the singly modified $hASL^{Lys3}_{UUU}$-t^6A_{37}.[53] The two solution structures differ dramatically in the anticodon (Fig. 8a). While the anticodon nucleosides in the singly modified construct are mostly unstacked, in $hASL^{Lys3}_{UUU}$-$mcm^5s^2U_{34}$;$ms^2t^6A_{37}$ the anticodon bases are clearly ordered into a well stacked conformation and exposed to the solvent for proper codon recognition. The anticodon stacking, abrupt backbone turn at U_{33} and the nicely ordered and stacked residues along the 3' side of the loop indicate that the doubly modified ASL has structural characteristics suggestive of a canonical conformation that would be significantly more favorable to ribosomal A-site binding.

Comparison of the crystal structures

A comparison of the crystal structures of the full length, fully modified $tRNA^{Lys3}_{UUU}$[54] to the co-crystal structures bound to synonymous codons in the ribosomal A-site reveals minor differences. This comparison strongly supports the hypothesis that modifications pre-structure tRNA`s anticodon domain for codon binding.[1]The crystal structures reported here, bound to AAA/G, are nearly superimposable, with a heavy atom rmsd of 0.45 Å (Supplementary Fig. S8,and Table S3a). The most notable difference between these two structures and the anticodon domain of the full length, fully modified $tRNA^{Lys3}_{UUU}$ occurs at the base of the stem. In the crystal structure of $tRNA^{Lys3}_{UUU}$, A_{31} forms a planar, stable base pair with U_{39},[54] but in the co-crystal structures on the ribosome, the A_{38} residue is rotated out of plane indicating a less stable base pair and possibly contributing to the opening of the loop. Interestingly, in the solution structure we observe that the $ms^2t^6A_{37}$ causes a slight perturbation of the C_{32}•A_{38} mismatch base pair by enhancing the stacking interaction of A_{38} with A_{37} and causing a displacement of ~0.4 Å. These data suggest that both ψ_{39} andms t^6A_{37} cooperatively extend the distance between C_{32} and A_{38} to abrogate the mismatch pair, forcing the loop into the open conformation necessary for a stable U-turn. Indeed, the distance and geometry between C 32 and A_{38} in all three crystal structures would not be amenable to a stable cross-loop interaction.

Comparison of the Solution and crystal structures

As expected from the Watson-Crick geometry of the U_{34}•G_3 wobble base pair, the crystal structures of the ASL bound to AAA and AAG codons were nearly identical (Supplementary Fig. S8). However, a superimposition of the NMR-derived solution structure of the $hASL^{Lys3}_{UUU}$-$mcm^5s^2U_{34}$;$ms^2t^6A_{37}$ with that of the crystal structure of the ASL region of the entire $tRNA^{54}$ and the co-crystal structure of $hASL^{Lys3}_{UUU}$-$mcm^5s^2U_{34}$;$ms^2t^6A_{37}$;ψ_{39} bound to the AAG codon indicates some salient differences (Fig. 9a, Supplementary Table S3c). The crystal structures show a very well defined U-turn conformation in which there is an abrupt change in direction at U_{33}.The anticodon bases are ideally stacked with their Watson-Crick faces solvent exposed and the bases on the 3' side of the loop form a very canonical stacking pattern (Supplementary Fig. S8). In contrast, in the solution structure, the common features of the U-turn are not evident and the structure is clearly dynamic (Fig. 9a). This feature is also evident in the thermal denaturation, where the doubly modified construct has a much lower hyperchromicity and enthalpy change than the triply modified $hASL^{Lys3}_{UUU}$-$mcm^5s^2U_{34}$;$ms^2t^6A_{37}$;ψ_{39} (Table 1). These are both

measures of the relative order of a molecule and indicate that these structural differences are empirical and not artifacts.

CONCLUSION

A lack of significant differences between the ASL of the full length tRNAcrystal structure and the co-crystals of the ASLs bound to the ribosome reveal that the functional binding results associated with using the truncated anticodon domain are a reasonable measure of the decoding capacity of the full length tRNA. It should also be noted that although an NMR-derived solution structure of the fully modified ASL was not obtained, it can be assumed that the addition of the ψ at position 39 would further drive the formation of a canonical U-turn in solution.[66,69] An induced fit model of decoding, in which the ASL would conform to a U-turn upon entering the ribosomal A-site is not consistent with the data due to the clear evidence from the crystal structure of the full length tRNA of a pre-structured, U-turn containing anticodon domain prior to entering the A-site.[54] Curiously, the high degree of structural conservation (rmsd = 0.65 − 0.77 Å, Supplementary Table S3a–c) between the crystal and the solution structures of the hASL$^{Lys3}_{UUU}$-mcm^{5}s^{2}U$_{34}$;ms^{2}t^{6}A$_{37}$;ψ$_{39}$ bound in the A-site suggests that in comparison, the anticodon domains of the partially modified *E. coli* ASLs incurred a degree of conformational change during codon recognition.[25]

The AAG codon binding of the hASL$^{Lys3}_{UUU}$-mcm^{5}s^{2}U$_{34}$;ms^{2}t^{6}A$_{37}$ exhibits an mcm^{5}s^{2}U$_{34}$•G3 pairing that is a Watson-Crick pair with three hydrogen bonds, one of which involves the s^2-modication. The hydrogen bond between the iminonitrogens of mcm^{5}s^{2}U$_{34}$ and G3 of the codon requires a keto-enoltautomerism similar to the mechanism by which cmo^{5}U$_{34}$ enables ASL^{Val3} to respond to all four codons in its degenerate box.[52] While the current mcm^{5}s^{2}U$_{34}$•G3 base pair structure agrees well with that of cmo^{5}U$_{34}$•G3.[52] it stands in stark contrast to the structure of mnm^{5}U$_{34}$•G3,[25] in which the modified U makes a three-centered hydrogen bond to G3 and partially stacks on U$_{35}$ (Fig. 7c). The equilibrium shift from the keto to enol tautomer inherent to these two modified nucleosides may suggest either a role of the cmo^5 or the s^2 and mcm^5 modifications in altering the electronic structure of the aromatic base or a local pH change in the environment in the immediate vicinity of the wobble base pair. It is critical to note that the mnm^{5}U$_{34}$ is missing the naturally-occurring 2-thio modification, so its stacking potential and electronic structure is not that which occurs in nature. The difference in binding modes could be due to the fact that the previous work is a different modification that does not affect the keto-enol equilibrium and thus does not allow a Watson-Crick base pair as for cmo^{5}U$_{34}$ and mcm^{5}s^{2}U$_{34}$ and that the observed structure is what will occur for the fully-modified ASL. The partially modified ASL$^{Lys}_{UUU}$-mnm^{5}U$_{34}$ binds the cognate AAA, but not the wobble codon AAG, while the unmodified *E. coli*ASL$^{Lys}_{UUU}$ binds neither codon.[8] We find it more likely that the previous, partially modified structure behaves differently from the fully modified mnm^{5}s^{2}U$_{34}$•G3, and that the fully modified structure would be very similar to the current structure. The thio modifications have been shown to be used to stack with adjacent rings for modifications at position-34 and 37, and were mnm^{5}U$_{34}$ to be fully thiolated, stacking on U$_{35}$ would require moving into Watson-Crick geometry. This is an excellent illustration of how finely tuned codon-anticodon interactions are, with the lack of one sulfur atom and presence of an oxygen disrupting the true structure of the codon-anticodon complex.[6]

Differences in modification between the bacterial and eukaryotic tRNA^{Lys}perhaps indicatethe co-evolution of anticodon modifications with codon bias and the use of less common tRNAisoacceptorsfor control of gene expression. Half of all bacteria have but the one tRNA^{Lys} with the UUU anticodon that reads the predominant codon AAA. The same tRNAreads the rarer codon AAG. In contrast, the additional isoacceptors tRNA$^{Lys1\&2}$ in mammalian cells have the anticodon CUU and respond only to AAG, the preferred lysine

codon by a factor of two. The amount of $tRNA^{Lys3}$ is only a third of the total amount of $tRNA^{Lys}$required for protein synthesis in mammalian cells. This leads one to the concept of codon bias being linked to tRNAisoacceptor abundance in the cell.[15]tRNA abundance, in turn is also correlated to environmental responses.[15]By pre-structuring the nucleoside geometry and backbone conformation, the $tRNA^{Lys3}$ modifications certainly alter the presentation of anticodon nucleosides for codon recognition. $tRNA^{Lys1,2}$ do not require t^6A_{37} for binding of the AAG codon,[8] but the anticodon modification t^6A_{37} that is common to all isoacceptors appears to be a recognition determinant for the lysyl-tRNAsynthetases. The difference in modifications between $tRNA^{Lys3}$ and $tRNA^{Lys1,2}$ implicate $tRNA^{Lys3}$ modifications in regulatinggene expression inmammalian cells through codon usage. Since lysine codons share a mixed codon box with the two asparagine codons, the major difference between isoacceptorsis located at the wobble position. Thus, the chemistries, structures and physical volumes of post-transcriptional modifications alter tRNA's anticodon conformation and restrict its dynamics for protein synthesis as had been proposed twenty years previously in a modified wobble hypothesis.[1]

METHODS AND MATERIALS

RNA sample preparation

In the solid-phase syntheses of the $hASL^{Lys3}_{UUU}$-$mcm^5s^2U_{34}$;$ms^2t^6A_{37}$ with and without ψ_{39}, the 5′-*O*-dimethoxytrityl- and 2′-*O*-t-butyldimethylsilyl-protecting groups were used for both modified and unmodified phosphoramidite monomers. The exocyclic amines of A, G and C were protected with the 4-*tert*-butylphenoxyacetyl (tac) group. The mcm^5s^2U phosphoramidite had no additional protecting groups. The ms^2t^6A phosphoramidite had the carboxyl group of the threonyl residue protected as a 4-nitrophenylethyl ester and the secondary hydroxyl group of the threonyl residue was protected as a *tert*-butyldimethylsilyl (TBDMS) ether.

Synthesis was performed on rC(tac) CPG (27 μmole and 31 μmole scale for non-ψ_{39} and ψ_{39} variants) and coupling was performed with 0.1 M monomer solutions and 0.3 M BTT in acetonitrile for 6 minutes (min) with U and C monomers, 7 min for A and G monomers, and for 10 min with the mcm^5s^2U and ms^2t^6A monomers. For standard RNA monomers 5 molar equivalents were used per coupling, but for the modified monomers only 3 equivalents were used. The capping step was performed for 2 min with tac anhydride. To prevent desulfurization, the oxidations were performed with 1 M cumenehydroperoxide in toluene for 3 min.

After assembly, the 5'-*O*-trityl group was left on. The dried support was treated with 10% DBU in THF under argon at 40°C to remove the cyanoethyl and 4-nitrophenylethyl protecting groups. The CPG was then washed twice with dry THF and treated with 10% DBU in methanol under argon for 18 hours at room temperature. The supernatant was removed and stored under argon. After washing with dry methanol, the washings and supernatant were combined and dried in a Speedvac. The residue was further dried under high vacuum (0.01–0.001 Torr) over separate containers of phosphorus pentoxide and potassium hydroxide pellets for 48 hours to remove residual DBU. The residue was then dissolved in triethyleneaminetri(hydrofluoride) under argon to cleave the TBDMS protecting groups and the DMTr from the 5'-terminal G. After quenching with water, the RNA was precipitated with 1-butanol and dried under vacuum. Purification was by preparative anion-exchange HPLC on a Source 15Q 10/10 column using a gradient of sodium chloride in a phosphate buffer containing 50 μM EDTA and 8 M urea. Desalting was performed on a Sephadex G25 column. Nucleoside composition analysis was conducted by HPLC with on-the-fly UV diode array spectroscopy.[70]

The ASLs were further purified by extensive dialysis (using Slide-A-Lyzer MINI Dialysis Units, 3.5K MWCO from Pierce) against 20 mM phosphate buffer (pH 6.8), 50 mM Na^+, and 50 mM K^+. The oligonucleotides were heated to 80 °C followed by slow cooling to form a solution homogeneous in ASL conformation. After cooling, the samples were lyophilized using a freeze-dryer (Thermo Savant SPD Speed Vac, Thermo Scientific) and then dissolved in 99.996% ^2H_2O or a 90% ^1H_2O+10% ^2H_2O mixture to give a final volume of 300 μL. Samples in ^2H_2O were re-dissolved in ^2H_2O at least twice more and lyophilized. NMR samples of the ASLs were generally at concentrations of 1.5 mM.

Ribosomal binding assay

The ribosomal binding assays consisted of reaction mixtures of purified *E. coli* (MRE 600) 70S ribosomes[42]and chemically synthesized mRNAs and ASLs. The 27-nt mRNA oligonucleotide sequences were derived from T4 gp32 mRNA[71] and were purchased from Dharmacon (ThermoFisher, Lafayette, CO). In order to study binding at the ribosomal A-site, the P-site needed to be blocked. Therefore, the mRNA was designed with the Methionine (Met) codon AUG at the P-site. The *E. coli*tRNA^{fMet} was then used to saturate the P-site. Possible secondary structure folding of each mRNA sequence was assessed with the program RNA Structure 4.2[72] and resulted in a low probability of any secondary structure that may obstruct binding of the mRNA to the ribosome. The mRNA sequences are as follows (Lys codons AAA and AAG are in bold and underlined):

1) 5'-GGCAAGGAGGUAAAAAUG**AAA**GCACGU-3';

2) 5'-GGCAAGGAGGUAAAAAUG**AAG**GCACGU-3'.

The 70S ribosomal subunits were isolated as previously described.[42] The ASLs were 5'-end ^{32}P-labeled using [γ-^{32}P] ATP (MP Biomedicals). Unlabeled ASLs in a range of concentrations (0–2.5μM) were mixed with insignificant, but radiochemically detectable amounts (2,000–5,000 CPM) of 5'-end, ^{32}P-labeled ASLs in a fixed ratio of unlabeled ASL to labeled ASL. The assay was performed in ribosomal binding buffer [50 mM HEPES, pH 7.0; 30 mMKCl; 70 mM NH4Cl; 1 mM DTT; 100 μM EDTA; 20 mM $MgCl_2$). Ribosomes (0.25μM) were activated by heating to 42°C, incubating for 10 min and then slowly cooled to 37°C. The ribosomes were programmed with 2.5 μM mRNA for 15 min at 37°C. The P-site was saturated with 1.25 μM*E. coli*tRNA^{fMet} (Sigma-Aldrich), which binds to AUG, for 15 min at 37°C; see underlined codons of the mRNA sequences above. Binding of ASL^{Lys3}_{UUU} to the A-site was allowed to proceed for 30 min at 37°C. The reaction mixtures (20μL each) were then placed on ice for 20 min, diluted with 100 μL buffer per reaction mixture, and filtered through nitrocellulose in a modified Whatman Schleicher and Schuell (Brentford, U.K.) 96-well filtration apparatus.[73] Prior to filtration of experimental samples, the nitrocellulose filter was equilibrated in binding buffer at 4°C for at least 20 min and each well of the filtration apparatus was washed with 100 μL of cold binding buffer. After filtration of reaction samples, each well was then washed twice with 100 μL of cold binding buffer. The nitrocellulose was blotted dry with Kimwipes (Kimberly-Clark), and the radioactivity was measured using a phosphorimager (Molecular Dynamics, GE Healthcare). Data were measured for radioactive intensity using ImageQuant (Amersham). Nonspecific binding was determined by the binding of ASLs to ribosomes without mRNA and subtracted from the experimental data. The final data is a result of at least two separate experiments, each done with samples in triplicate, *i.e.* at least six results for each binding point.

Thermal denaturation

The thermal stabilities of the ASLs were monitored using a Varian Cary 3 UV-visible spectrophotometer (Agilent) controlled with WinUV version 3.00 software. All samples were first adjusted to an absorbance of ~0.2 OD units at 260 nm in 20 mMsodium/potassium

phosphate buffer (10 mM Na_2HPO_4 and 10 mM KH_2PO_4, pH 6.8). Absorbance at 260nm was measured over the temperature range of 5°C to 95°C. The temperature was ramped at 1°C/min and data was collected at a rate of 1 data point per minute, averaged over 2 seconds. Thermodynamic parameters and melting temperatures were calculated from the melt profiles using MeltWin v3.5. All data were baseline corrected using a control containing buffer only.

Circular dichroism

Circular dichroism spectra were collected on a Jasco J600 spectropolarimeter. All samples were adjusted to ~0.2 OD at 260nm in 20mM sodium/potassium phosphate buffer (10 mM Na_2HPO_4 and 10 mM KH_2PO_4, pH 6.8) prior to CD analysis and analyzed in a 1 cm path length quartz cuvette. Samples were temperature controlled to 25°C during data collection. All data were baseline corrected using a control containing buffer only.

NMR experiments

Bruker DRX500 and Varian Inova-600 instruments were used to conduct the experiments. NMR data were processed with either XWINNMR (Bruker Inc., Rheinstetten, Germany) or NMRPipe,[74] and the analysis was conducted with SPARKY.[75] WATERGATE[76] method was used to suppress the water signal resulting from the samples prepared in ^{1}H2O whereas a low-power presaturation technique was used for samples dissolved in ^2H_2O. NOESY[77] experiments of the samples in ^{1}H2O were performed at low temperatures (2, 5, and 10 °C) to observe the exchangeable proton resonances. For NMR resonance assignments:^{1}H-^{1}H-COSY, ^{1}H-^{1}H-DQF-COSY, ^{1}H-^{1}H-TOCSY, natural abundance ^{1}H-^{13}C HSQC, and ^{1}H-^{31}P HETCOR experiments were performed.[49] To achieve structures determination, NOESY experiments were conducted in ^2H_2O with different mixing times (50, 75, 100, 200, 300, and 400 ms) at 22 °C without removing the samples from the magnet. The spectra were acquired with spectral widths of 5000 Hz in both dimensions, 1024 points in t_2, 360 points with 64 scans per block in t_1, and a recycle delay of 1.5 s. The FIDs were processed with 60° phase-shifted sine bell apodization functions and third-degree polynomial baseline correction in both dimensions. To improve the digital resolution for the cross-peak integration, the FIDs were zerofilled to 2048 × 2048 points.

Structure Determination

Structure calculations were performed using CNS and were based on published protocols.[47,78,79]The backbone and the ribose torsion angles were restrained to be within ±15° of the standard A-form values. NOESY mixing time studies also provided distance restraints between nonexchangeable protons in the loop region. The NOE cross-peaks were integrated by using the peak fitting Gaussian function and volume integration in SPARKY. The distances were determined and normalized to the non-overlapped pyrimidine H5–H6 cross-peaks with a distance of 2.44 Å. Upper and lower bonds were assigned to ± 20% of the calculated distances. The distances involving the unresolved protons, i.e., methyls of $ms^2t^6A_{37}$ and $mcm^5s^2U_{34}$ as well as its methylene group, were subjected to the pseudoatom correction automatically computed by CNS. Residues with non-observable H1′–H2′ cross-peaks on the DQF-COSY spectra or with $^3J_{H1'–H2'}$ values of <3 Hz were restrained to the C3′-*endo* conformation, whereas in those with ^3JH1′–H2′ values appearing to be between 4 and 5 Hz, the ribose was left unconstrained. The α and ζ torsion angles were restrained to exclude the *trans* conformation. The β, ε, and γangles were restrained on the basis of the ^{1}H-^{31}P HETCOR spectra as previously described.[44,49] The structures were analyzed using 3DNA.[80]

Crystallographic methods

Purification, crystallization and cryoprotection of *Thermusthermophilus* 30S ribosomal subunits was conducted exactly as has been described.[81] The mRNA oligonucleotides were chemically synthesized (Dharmacon,ThermoFisher, Lafayette, CO) with the sequences 5'-AA(A/G)AAA-3' (codons underlined). After cryoprotection, the empty crystals were soaked in cryoprotection solution augmented with 80 μM paromomycin, 300 μM ASL and 300 μM mRNA oligonucleotide for at least 48 hours. Crystals were flash-cooled by plunging into liquid nitrogen and stored for data collection.

Crystals were pre-screened at European Synchrotron Radiation Facility (ESRF, Grenoble, France) beamline ID14-2 and data was collect at ESRF beamline ID14-4. Processing was performed using XDS,[82] CCP4 (Collaborative Computational Project Number 4:1994) was used for format manipulation, COOT[83] for visualization and model building, CNS 1.2[79] for refinement, HIC-Up[84] for novel constraints generation, 3DNA[85] for RNA analysis and PyMOL[86] for figure production.

Supplementary Material

Refer to Web version on PubMed Central for supplementary material.

Acknowledgments

The authors thank W. D. Graham for purifying the ASLs and G. Björk for conducting the HPLC nucleoside composition analysis. We thank the members of the laboratory of V. Ramakrishnan for their support in conducting the X-ray crystallography. Specifically, A. Kelley for purification and crystallization of 30S ribosomal subunits, C.M. Dunham, S. Petry and A. Weixlbaumer for assistance with data collection, G. Leonard, J. McCarthy and R. Ravelli for assistance with data collection on ESRF ID14. We thank Caren Stark and Jen Montimurro for their help in revising the manuscript. In addition, the authors acknowledge the support of grants from the National Institutes of Health, the National Science Foundation, and the North Carolina Biotechnology Center to P.F.A. (2RO1-GM23037, MCB0548602 and MRG 1102/Agris,respectively) and a grant from the National Science Center, Poland (1306/B/H03/2011/40)to G.L.

Abbreviations

ASL	anticodon stem and loop
hASL$^{Lys3}_{UUU}$	ASL of human lysine tRNAisoaccepting species 3 with anticodon UUU
CD	circular dichroismspectropolarimetry
mcm^{5}s^{2}U$_{34}$	5-methoxycarbonylmethyl-2-thiouridine at position 34
ms^{2}t^{6}A$_{37}$	2-methylthio-*N*^{6}-threonylcarbamoyladenosine at position 37
HPLC	high performance liquid chromatography
NOE	nuclear Overhauser effect
Tm	temperature at the mid-point in the UV-monitored major thermal transition

REFERENCES

1. Agris PF. Wobble position modified nucleosides evolved to select transfer RNA codon recognition: a modified-wobble hypothesis. Biochimie. 1991; 73:1345–1349. [PubMed: 1799628]
2. Agris PF, Vendeix FAP, Graham WD. tRNA's wobble decoding of the genome: 40 years of modification. J Mol Biol. 2007; 366:1–13. [PubMed: 17187822]
3. Nishimura S, Watanabe K. The discovery of modified nucleosides from the early days to the present: a personal perspective. J. Biosci. 2006; 31:465–475. [PubMed: 17206067]

4. Yarus M. Translational efficiency of transfer RNA's: uses of an extended anticodon. Science. 1982; 218:646–652. [PubMed: 6753149]
5. Cantara WA, Crain PF, Rozenski J, McCloskey JA, Harris KA, Zhang X, Vendeix FAP, Fabris D, Agris PF. The RNA Modification Database, RNAMDB: 2011 update. Nucleic Acids Res. 2011; 39:D195–201. [PubMed: 21071406]
6. Ashraf SS, Sochacka E, Cain R, Guenther R, Malkiewicz A, Agris PF. Single atom modification (O-->S) of tRNA confers ribosome binding. RNA. 1999; 5:188–194. [PubMed: 10024171]
7. Yarian C, Townsend H, Czestkowski W, Sochacka E, Malkiewicz AJ, Guenther R, Miskiewicz A, Agris PF. Accurate translation of the genetic code depends on tRNA modified nucleosides. J Biol Chem. 2002; 277:16391–16395. [PubMed: 11861649]
8. Yarian C, Marszalek M, Sochacka E, Malkiewicz A, Guenther R, Miskiewicz A, Agris PF. Modified nucleoside dependent Watson-Crick and wobble codon binding by $tRNA^{Lys}_{UUU}$ species. Biochemistry. 2000; 39:13390–13395. [PubMed: 11063576]
9. Hagervall TG, Pomerantz SC, McCloskey JA. Reduced misreading of asparagine codons by *Escherichia coli* $tRNA^{Lys}$ with hypomodified derivatives of 5-methylaminomethyl-2-thiouridine in the wobble position. J. Mol. Biol. 1998; 284:33–42. [PubMed: 9811540]
10. Lim VI. Analysis of action of wobble nucleoside modifications on codonanticodon pairing within the ribosome. J. Mol. Biol. 1994; 240:8–19. [PubMed: 8021943]
11. Stuart JW, Koshlap KM, Guenther R, Agris PF. Naturally-occurring modification restricts the anticodon domain conformational space of $tRNA^{Phe}$. J Mol Biol. 2003; 334:901–918. [PubMed: 14643656]
12. Krüger MK, Pedersen S, Hagervall TG, Sørensen MA. The modification of the wobble base of $tRNA^{Glu}$ modulates the translation rate of glutamic acid codons *in vivo*. J. Mol. Biol. 1998; 284:621–631. [PubMed: 9826503]
13. Tamura K, Himeno H, Asahara H, Hasegawa T, Shimizu M. *In vitro* study of *E.coli* $tRNA^{Arg}$ and $tRNA^{Lys}$ identity elements. Nucleic Acids Res. 1992; 20:2335–2339. [PubMed: 1375736]
14. Björk GR, Durand JM, Hagervall TG, Leipuviene R, Lundgren HK, Nilsson K, Chen P, Qian Q, Urbonavicius J. Transfer RNA modification: influence on translational frameshifting and metabolism. FEBS Lett. 1999; 452:47–51. [PubMed: 10376676]
15. Gustilo EM, Vendeix FA, Agris PF. tRNA's modifications bring order to gene expression. Curr. Opinion in Microbiol. 2008; 11:134–140.
16. Urbonavicius J, Qian Q, Durand JM, Hagervall TG, Björk GR. Improvement of reading frame maintenance is a common function for several tRNA modifications. EMBO J. 2001; 20:4863–4873. [PubMed: 11532950]
17. Brierley I, Meredith MR, Bloys AJ, Hagervall TG. Expression of a coronavirus ribosomal frameshift signal in *Escherichia coli*: influence of tRNA anticodon modification on frameshifting. J Mol Biol. 1997; 270:360–373. [PubMed: 9237903]
18. Agris PF. Bringing order to translation: the contributions of transfer RNA anticodon-domain modifications. EMBO Rep. 2008; 9:629–635. [PubMed: 18552770]
19. Barat C, Lullien V, Schatz O, Keith G, Nugeyre MT, Grüninger-Leitch F, Barré-Sinoussi F, LeGrice SF, Darlix JL. HIV-1 reverse transcriptase specifically interacts with the anticodon domain of its cognate primer tRNA. EMBO J. 1989; 8:3279–3285. [PubMed: 2479543]
20. Bilbille Y, Vendeix FAP, Guenther R, Malkiewicz A, Ariza X, Vilarrasa J, Agris PF. The structure of the human $tRNA^{Lys3}$ anticodon bound to the HIV genome is stabilized by modified nucleosides and adjacent mismatch base pairs. Nucleic Acids Res. 2009; 37:3342–3353. [PubMed: 19324888]
21. Isel C, Marquet R, Keith G, Ehresmann C, Ehresmann B. Modified nucleotides of $tRNA^{Lys3}$ modulate primer/template loop-loop interaction in the initiation complex of HIV-1 reverse transcription. J. Biol. Chem. 1993; 268:25269–25272. [PubMed: 7503978]
22. Tisné C, Rigourd M, Marquet R, Ehresmann C, Dardel F. NMR and biochemical characterization of recombinant human $tRNA^{Lys3}$ expressed in *Escherichia coli*: identification of posttranscriptional nucleotide modifications required for efficient initiation of HIV-1 reverse transcription. RNA. 2000; 6:1403–1412. [PubMed: 11073216]
23. Jühling F, Mörl M, Hartmann RK, Sprinzl M, Stadler PF, Pütz J. tRNAdb 2009: compilation of tRNA sequences and tRNA genes. Nucleic Acids Res. 2009; 37:D159–162. [PubMed: 18957446]

24. Chakraburtty K, Steinschneider A, Case RV, Mehler AH. Primary structure of $tRNA^{Lys}$ of *E. coli* B. Nucleic Acids Res. 1975; 2:2069–2075. [PubMed: 802509]
25. Murphy FV, Ramakrishnan V, Malkiewicz A, Agris PF. The role of modifications in codon discrimination by $tRNA^{Lys}_{UUU}$. Nature Struct. Biol. 2004; 11:1186–1191.
26. Sundaram M, Durant PC, Davis DR. Hypermodified nucleosides in the anticodon of $tRNA^{Lys}$ stabilize a canonical U-turn structure. Biochemistry. 2000; 39:12575–12584. [PubMed: 11027137]
27. Madore E, Florentz C, Giegé R, Sekine S, Yokoyama S, Lapointe J. Effect of modified nucleotides on *Escherichia coli* $tRNA^{Glu}$ structure and on its aminoacylation by glutamyl-tRNA synthetase. Predominant and distinct roles of the mnm^5 and s^2 modifications of U34. Eur. J. Biochem. 1999; 266:1128–1135. [PubMed: 10583410]
28. Seno T, Agris PF, Söll D. Involvement of the anticodon region of *Escherichia coli* $tRNA^{Gln}$ and $tRNA^{Glu}$ in the specific interaction with cognate aminoacyltRNA synthetase. Alteration of the 2-thiouridine derivatives located in the anticodon of the tRNAs by BrCN or sulfur deprivation. Biochim. Biophys. Acta. 1974; 349:328–338. [PubMed: 4366808]
29. Sylvers LA, Rogers KC, Shimizu M, Ohtsuka E, Söll D. A 2-thiouridine derivative in $tRNA^{Glu}$ is a positive determinant for aminoacylation by *Escherichia coli* glutamyl-tRNA synthetase. Biochemistry. 1993; 32:3836–3841. [PubMed: 8385989]
30. Krüger MK, Sørensen MA. Aminoacylation of hypomodified $tRNA^{Glu}$ *in vivo*. J. Mol. Biol. 1998; 284:609–620. [PubMed: 9826502]
31. Powers DM, Peterkofsky A. Biosynthesis and specific labeling of N-(purin-6-ylcarbamoyl)threonine of *Escherichiacoli* transfer RNA. Biochem. Biophys. Res. Commun. 1972; 46:831–838. [PubMed: 4550699]
32. Raba M, Limburg K, Burghagen M, Katze JR, Simsek M, Heckman JE, Rajbhandary UL, Gross HJ. Nucleotide sequence of three isoaccepting lysine tRNAs from rabbit liver and SV40-transformed mouse fibroblasts. Eur. J. Biochem. 1979; 97:305–318. [PubMed: 225173]
33. Baczynskyj L, Biemann K, Fleysher MH, Hall RH. Synthesis of 2-thio-5-carboxymethyluridine methyl ester: a component of transfer RNA. Can. J. Biochem. 1969; 47:1202–1203. [PubMed: 5364028]
34. Baczynskyj L, Biemann K, Hall RH. Sulfur-containing nucleoside from yeast transfer ribonucleic acid: 2-thio-5(or 6)-uridine acetic acid methyl ester. Science. 1968; 159:1481–1483. [PubMed: 5732490]
35. Yamaizumi Z, Nishimura H, Limburg K, Raba M, Gross HJ, Crain PF, McCloskey JA. Structure elucidation by high resolution mass spectrometry of a highly modified nucleoside from mammalian transfer RNA. N-[(9-.beta.-D-Ribofuranosyl-2-methylthiopurin-6-yl)carbamoyl]threonine. J. Am. Chem. Soc. 1979; 101:2224–2225.
36. Cohn WE. 5-Ribosyl uracil, a carbon-carbon ribofuranosyl nucleoside in ribonucleic acids. Biochim. Biophys. Acta. 1959; 32:569–571. [PubMed: 13811055]
37. Yu CT, Allen FW. Studies on an isomer of uridine isolated from ribonucleic acids. Biochim. Biophys. Acta. 1959; 32:393–406. [PubMed: 13846687]
38. Lustig F, Elias P, Axberg T, Samuelsson T, Tittawella I, Lagerkvist U. Codon reading and translational error. Reading of the glutamine and lysine codons during protein synthesis in vitro. J. Biol. Chem. 1981; 256:2635–2643. [PubMed: 6782093]
39. Johansson MJO, Esberg A, Huang B, Björk GR, Byström AS. Eukaryotic wobble uridine modifications promote a functionally redundant decoding system. Mol. Cell. Biol. 2008; 28:3301–3312. [PubMed: 18332122]
40. McCrate NE, Varner ME, Kim KI, Nagan MC. Molecular dynamics simulations of human $tRNA^{Lys,3}_{UUU}$: the role of modified bases in mRNA recognition. Nucleic Acids Res. 2006; 34:5361–5368. [PubMed: 17012271]
41. Durant PC, Bajji AC, Sundaram M, Kumar RK, Davis DR. Structural effects of hypermodified nucleosides in the *Escherichia coli* and human $tRNA^{Lys}$ anticodon loop: The effect of nucleosides s^2U, mcm^5U, mcm^5s^2U, mnm^5s^2U, t^6A, and ms^2t^6A. Biochemistry. 2005; 44:8078–8089. [PubMed: 15924427]

42. Phelps SS, Jerinic O, Joseph S. Universally conserved interactions between the ribosome and the anticodon stem-loop of A site tRNA important for translocation. Mol. Cell. 2002; 10:799–807. [PubMed: 12419224]
43. Watanabe K, Oshima T, Nishimura S. CD spectra of 5-methyl-2-thiouridine in tRNA-Met-f from an extreme thermophile. Nucleic Acids Res. 1976; 3:1703–1713. [PubMed: 967669]
44. Varani G, Adoul-ela F, Allain FHT. NMR investigation of RNA structure. Progr. Nuclear Magnetic Resonance Spectroscopy. 1996; 29:51–127.
45. Wijmenga S, Buuren BNM. The use of NMR methods for conformational studies of nucleic acids. Progr. Nuclear Magnetic Resonance Spectroscopy. 1998; 32:287–387.
46. Cabello-Villegas J, Tworowska I, Nikonowicz EP. Metal ion stabilization of the U-turn of the $A_{37}N^6$-dimethylallyl-modified anticodon stem-loop of *Escherichia coli* $tRNA^{Phe}$. Biochemistry. 2003; 43:55–66. [PubMed: 14705931]
47. Vendeix FAP, Dziergowska A, Gustilo EM, Graham WD, Sproat B, Malkiewicz A, Agris PF. Anticodon domain modifications contribute order to tRNA for ribosome-mediated codon binding. Biochemistry. 2008; 47:6117–6129. [PubMed: 18473483]
48. Schweisguth DC, Moore PB. On the conformation of the anticodon loops of initiator and elongator methionine tRNAs. J. Mol. Biol. 1997; 267:505–519. [PubMed: 9126834]
49. Varani G, Tinoco I. RNA structure and NMR spectroscopy. Q. Rev. Biophys. 1991; 24:479–532. [PubMed: 1723809]
50. Saenger, W. Principles of Nucleic Acid Structure. Springer-Verlag; New York: 1983.
51. Ogle JM, Brodersen DE, Clemons WM, Tarry MJ, Carter AP, Ramakrishnan V. Recognition of cognate transfer RNA by the 30S ribosomal subunit. Science. 2001; 292:897–902. [PubMed: 11340196]
52. Weixlbaumer A, Murphy FV, Dziergowska A, Malkiewicz A, Vendeix FAP, Agris PF, Ramakrishnan V. Mechanism for expanding the decoding capacity of transfer RNAs by modification of uridines. Nature Struct. Biol. 2007; 14:498–502.
53. Stuart JW, Gdaniec Z, Guenther R, Marszalek M, Sochacka E, Malkiewicz A, Agris PF. Functional anticodon architecture of human $tRNA^{Lys3}$ includes disruption of intraloop hydrogen bonding by the naturally occurring amino acid modification, t^6A. Biochemistry. 2000; 39:13396–13404. [PubMed: 11063577]
54. Bénas P, Bec G, Keith G, Marquet R, Ehresmann C, Ehresmann B, Dumas P. The crystal structure of HIV reverse-transcription primer tRNA(Lys,3) shows a canonical anticodon loop. RNA. 2000; 6:1347–1355. [PubMed: 11073212]
55. Mazumdar SK, Saenger W. Molecular structure of poly-2-thiouridylic acid, a double helix with non-equivalent polynucleotide chains. J. Mol. Biol. 1974; 85:213–219. [PubMed: 4836283]
56. Phelps SS, Malkiewicz A, Agris PF, Joseph S. Modified nucleotides in $tRNA^{Lys}$ and $tRNA^{Val}$ are important for translocation. J Mol Biol. 2004; 338:439–444. [PubMed: 15081802]
57. Smith WS, Sierzputowska-Gracz H, Sochacka E, Malkiewicz A, Agris PF. Chemistry and structure of modified uridine dinucleosides are determined by thiolation. J. Amer. Chem. Soc. 1992; 114:7989–7997.
58. Yokoyama S, Watanabe T, Murao K, Ishikura H, Yamaizumi Z, Nishimura S, Miyazawa T. Molecular mechanism of codon recognition by tRNA species with modified uridine in the first position of the anticodon. Proc. Natl. Acad. Sci. U.S.A. 1985; 82:4905–4909. [PubMed: 3860833]
59. Guyader M, Emerman M, Sonigo P, Clavel F, Montagnier L, Alizon M. Genome organization and transactivation of the human immunodeficiency virus type 2. Nature. 1987; 326:662–669. [PubMed: 3031510]
60. Wain-Hobson S, Sonigo P, Danos O, Cole S, Alizon M. Nucleotide sequence of the AIDS virus, LAV. Cell. 1985; 40:9–17. [PubMed: 2981635]
61. Sanchez-Pescador R, Power MD, Barr PJ, Steimer KS, Stempien MM, Brown-Shimer SL, Gee WW, Renard A, Randolph A, Levy JA, et al. Nucleotide sequence and expression of an AIDS-associated retrovirus (ARV-2). Science. 1985; 227:484–492. [PubMed: 2578227]
62. Vendeix FAP, Munoz AM, Agris PF. Free energy calculation of modified base-pair formation in explicit solvent: A predictive model. RNA. 2009; 15:2278–2287. [PubMed: 19861423]

63. Agris PF, Sierzputowska-Gracz H, Smith W, Malkiewicz A, Sochacka E, Nawrot B. Thiolation of uridine carbon-2 restricts the motional dynamics of the transfer RNA wobble position nucleoside. J. Amer. Chem. Soc. 1992; 114:2652–2656.
64. Sierzputowska-Gracz H, Sochacka E, Malkiewicz A, Kuo K, Gehrke CW, Agris PF. Chemistry and structure of modified uridines in the anticodon, wobble position of transfer RNA are determined by thiolation. J Am Chem Soc. 1987; 109:7171–7177.
65. Dao V, Guenther R, Malkiewicz A, Nawrot B, Sochacka E, Kraszewski A, Jankowska J, Everett K, Agris PF. Ribosome binding of DNA analogs of tRNA requires base modifications and supports the “extended anticodon”. Proc. Natl. Acad. Sci. U.S.A. 1994; 91:2125–2129. [PubMed: 7510886]
66. Durant PC, Davis DR. Stabilization of the anticodon stem-loop of $tRNA^{Lys,3}$ by an A+-C base-pair and by pseudouridine. J Mol Biol. 1999; 285:115–131. [PubMed: 9878393]
67. Ashraf SS, Guenther RH, Ansari G, Malkiewicz A, Sochacka E, Agris PF. Role of modified nucleosides of yeast tRNA(Phe) in ribosomal binding. Cell Biochem Biophys. 2000; 33:241–252. [PubMed: 11325044]
68. Bajji AC, Davis DR. Synthesis of the $tRNA^{Lys,3}$ anticodon stem-loop domain containing the hypermodified ms^2t^6A nucleoside. J. Org. Chem. 2002; 67:5352–5358. [PubMed: 12126427]
69. Yarian CS, Basti MM, Cain RJ, Ansari G, Guenther RH, Sochacka E, Czerwinska G, Malkiewicz A, Agris PF. Structural and functional roles of the N1- and N3-protons of Y at tRNA's position 39. Nucleic Acids Res. 1999; 27:3543–3549. [PubMed: 10446245]
70. Davis GE, Gehrke CW, Kuo KC, Agris PF. Major and modified nucleosides in tRNA hydrolysates by high-performance liquid chromatography. J. Chromatogr. 1979; 173:281–298. [PubMed: 94916]
71. Fahlman RP, Dale T, Uhlenbeck OC. Uniform binding of aminoacylated transfer RNAs to the ribosomal A and P sites. Mol Cell. 2004; 16:799–805. [PubMed: 15574334]
72. Mathews DH, Turner DH, Zuker M. RNA secondary structure prediction. Curr. Protoc. Nucleic Acid Chem. 2007; Chapter 11(Unit 11):12.
73. Wong I, Lohman TM. A double-filter method for nitrocellulose-filter binding: application to protein-nucleic acid interactions. Proc Natl Acad Sci USA. 1993; 90:5428–5432. [PubMed: 8516284]
74. Delaglio F, Grzesiek S, Vuister G, Zhu G, Pfeifer J, Bax A. NMRPipe: A multidimensional spectral processing system based on UNIX pipes. J Biomol NMR. 1995; 6:277–293. [PubMed: 8520220]
75. Goddard, TD.; Kneller, DG. SPARKY3. San Franscisco, California, USA: 2007.
76. Piotto M, Saudek V, Sklenář V. Gradient-tailored excitation for single-quantum NMR spectroscopy of aqueous solutions. J. Biomol. NMR. 1992; 2:661–665. [PubMed: 1490109]
77. Kumar A, Ernst R, Wuthrich K. A two-dimensional nuclear Overhauser enhancement (2D NOE) experiment for the elucidation of complete proton-proton cross-relaxation networks in biological macromolecules. Biochem. Biophys. Res. Commun. 1980; 95:1–6. [PubMed: 7417242]
78. Stein EG, Rice LM, Brünger AT. Torsion-angle molecular dynamics as a new efficient tool for NMR structure calculation. J Magn Reson. 1997; 124:154–164. [PubMed: 9424305]
79. Brünger AT, Adams PD, Clore GM, DeLano WL, Gros P, Grosse-Kunstleve RW, Jiang JS, Kuszewski J, Nilges M, Pannu NS, Read RJ, Rice LM, Simonson T, Warren GL. Crystallography & NMR system: A new software suite for macromolecular structure determination. Acta Crysallogr. D Biol. Crystallogr. 1998; 54:905–921.
80. Lu XJ, Olson WK. 3DNA: a software package for the analysis, rebuilding and visualization of three-dimensional nucleic acid structures. Nucleic Acids Res. 2003; 31:5108–5121. [PubMed: 12930962]
81. Clemons WM, Brodersen DE, McCutcheon JP, May JL, Carter AP, Morgan-Warren RJ, Wimberly BT, Ramakrishnan V. Crystal structure of the 30S ribosomal subunit from *Thermus thermophilus*: purification, crystallization and structure determination. J. Mol. Biol. 2001; 310:827–843. [PubMed: 11453691]
82. Kabsch W. Automatic processing of rotation diffraction data from crystals of initially unknown symmetry and cell constants. J. Appl. Crystallogr. 1993; 26:795–800.

83. Emsley P, Cowtan K. Coot: model-building tools for molecular graphics. Acta Crysallogr. D Biol. Crystallogr. 2004; 60:2126–2132.

84. Kleywegt GJ, Jones TA. Databases in protein crystallography. Acta Crystallogr. D Biol. Crystallogr. 1998; 54:1119–1131. [PubMed: 10089488]

85. Lu X-J, Olson WK. 3DNA: a versatile, integrated software system for the analysis, rebuilding and visualization of three-dimensional nucleic-acid structures. Nature Protocols. 2008; 3:1213–1227.

86. DeLano, WL. Pymol. Delano Scientific. San Carlos, California, USA: 2006.

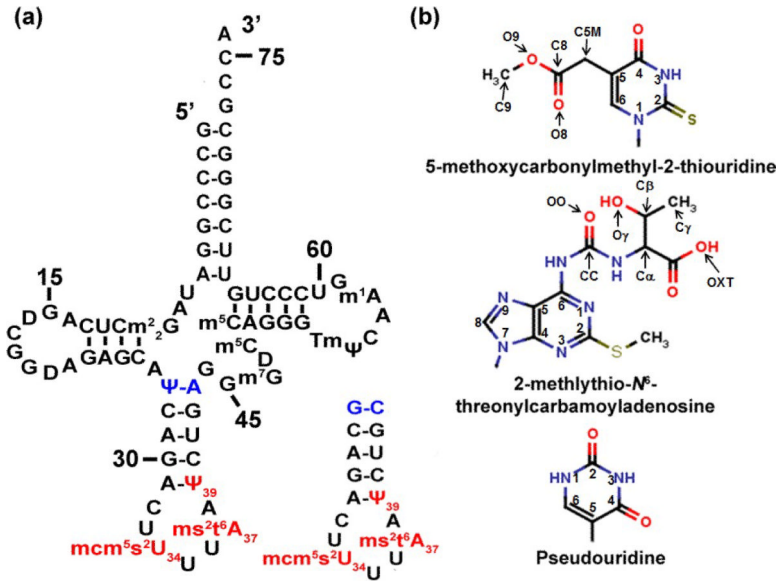

Figure 1.

Human $tRNA^{Lys3}_{UUU}$, its anticodon stem and loop domain and its modified nucleosides. **(a)** Sequence and secondary structure of human $tRNA^{Lys3}$ ($htRNA^{Lys3}_{UUU}$) with all of its known modified nucleosides: N^2,N^2-dimethylguanosine at position 10, $m^2{}_2G_{10}$; dihydrouridine at positions 16, 20 and 48, D; pseudouridine-27 (ψ), 39 (ψ) and 55 (ψ); 5-methoxycarbonylmethyl-2-thiouridine-34, **$mcm^5s^2U_{34}$**; 2-methylthio-N^6-threonylcarbamoyladenosine-37, **$ms^2t^6A_{37}$**; N^7-methylguanosine, m^7G; 5-methylcytidine at positions 48 and 49, m^5C; 2'-O-methylribothymidine (2'-O-methyl-5-methyluridine), Tm; N^1-methyladenosine-58, m^1A. The modifications,**$mcm^5s^2U_{34}$, $ms^2t^6A_{37}$** and **$ψ_{39}$**are in red. The ASLs were synthesized with a G_{27}•C_{34} terminal base pair instead of the $ψ_{27}$•A_{43} in order to stabilize the stem. **(b)** Chemical structures of the modified nucleosides within the anticodon stem and loop domain of $htRNA^{Lys3}_{UUU}$: $mcm^5s^2U_{34}$; $ms^2t^6A_{37}$; and $ψ_{39}$.

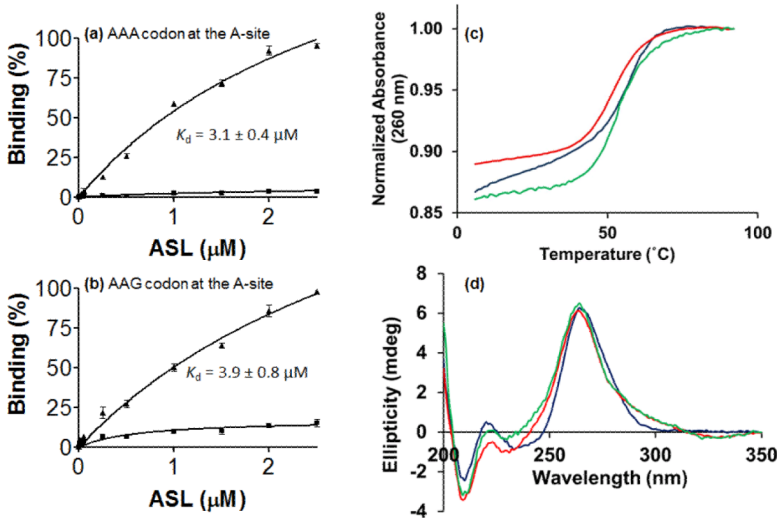

Figure 2.

Ribosome-mediated codon binding and thermodynamic analysis.**(a)** Equilibrium binding of the cognate codon **(a)** AAA and **(b)** AAG in the aminoacyl, or A-site of the *Escherichia coli* 70S ribosome by $hASL^{Lys3}_{UUU}$-$mcm^5s^2U_{34}$;$ms^2t^6A_{37}$ (▲) and the unmodified $hASL^{Lys3}_{UUU}$ (■). **(c)** UV-monitored, thermal denaturations of the $hASL^{Lys3}_{UUU}$-$mcm^5s^2U_{34}$;$ms^2t^6A_{37}$ (**red**,-—), $hASL^{Lys3}_{UUU}$-$mcm^5s^2U_{34}$;$ms^2t^6A_{37}$;ψ_{39} (**green**,—) and the unmodified $hASL^{Lys3}_{UUU}$ (**blue**,—). Thermal denaturations/renaturations are the averages of three separate experiments. Results are presented after baseline correction and normalization to 1.00 at maximum absorbance. Thermodynamic parameters extracted from these experiments are found in Table 1 and reflect errors as one standard deviation. **(d)** Circular dichroism (CD) spectra of the $hASL^{Lys3}_{UUU}$-$mcm^5s^2U_{34}$;$ms^2t^6A_{37}$ (**red**,-—), $hASL^{Lys3}_{UUU}$-$mcm^5s^2U_{34}$;$ms^2t^6A_{37}$;ψ_{39} (**green**,—) and the unmodified $hASL^{Lys3}_{UUU}$ (**blue**,—). Spectra were collected at 25 °C, and are shown as the averages of three separate experiments after baseline correction.

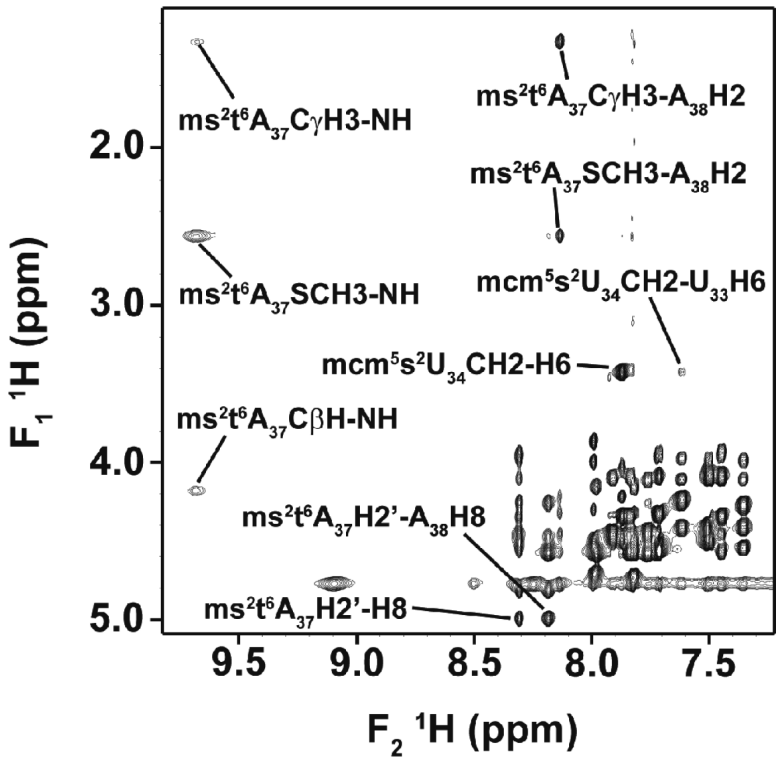

Figure 3.

Two dimensional homonuclear (^{1}H-^{1}H) NOESYNMR spectrum of hASL$^{Lys3}_{UUU}$-mcm^{5}s^{2}U$_{34}$;ms^{2}t^{6}A$_{37}$. The spectrum demonstrates the unambiguous identification ofthe modified nucleoside residues. NOE cross-peaks were observed between the atoms of mcm^{5}s^{2}U$_{34}$ and ms^{2}t^{6}A$_{37}$ and those of the residues that are in their respective vicinity.This spectrum of hASL$^{Lys3}_{UUU}$-mcm^{5}s^{2}U$_{34}$;ms^{2}t^{6}A$_{37}$ (1.5 mM in 90% ^1H_2O + 10% ^2H_2O at pH 6.8, 295 °K) was recorded with a mixing time of 400 ms and at 500 MHz.

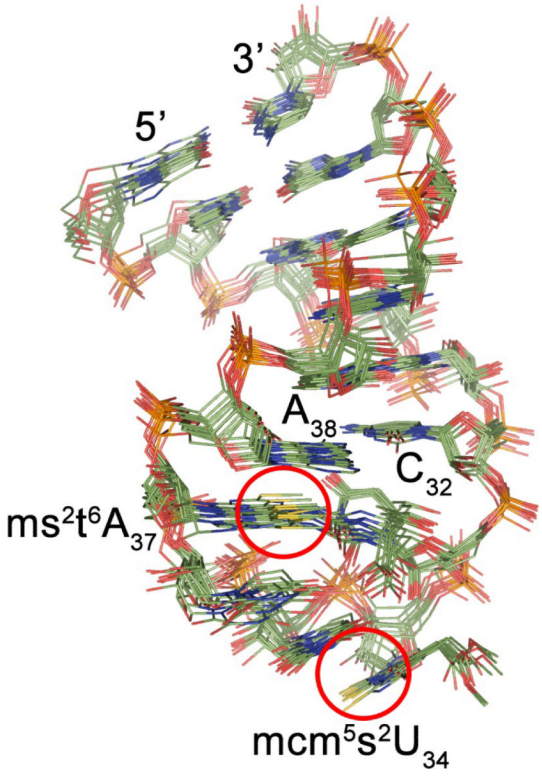

Figure 4.

Solution structure of hASL$^{Lys3}_{UUU}$-mcm^{5}s^{2}U$_{34}$;ms^{2}t^{6}A$_{37}$. Ensemble of the ten lowest energy structures of hASL$^{Lys3}_{UUU}$-mcm^{5}s^{2}U$_{34}$;ms^{2}t^{6}A$_{37}$ obtained from the NMR-derived, restrained molecular dynamics. The pairwise rmsd for all atoms is 0.82 ± 0.20 Å from the average structure. The locations of the modified residues are indicated by red circles for clarity.

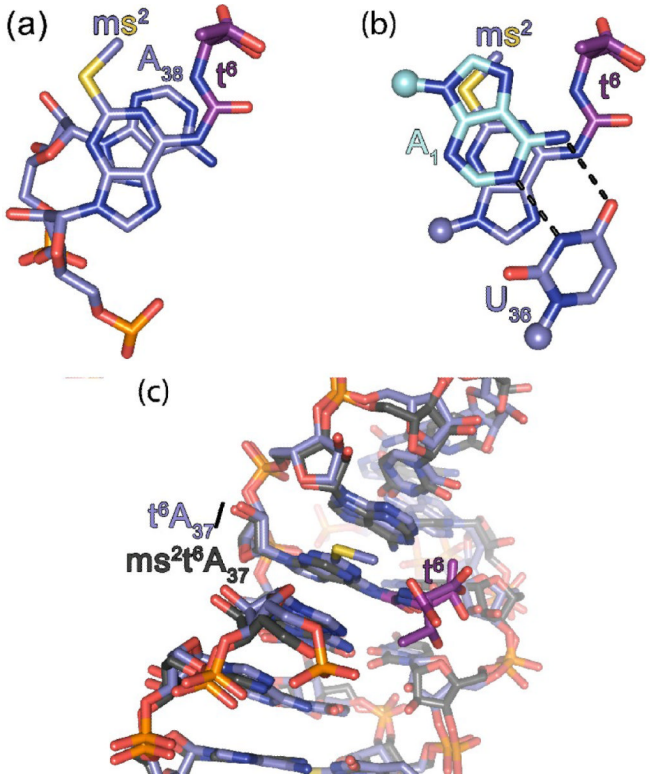

Figure 5.

Crystallographic structures of hASL$^{Lys3}_{UUU}$-mcm^{5}s^{2}U$_{34}$;ms^{2}t^{6}A$_{37}$;ψ$_{39}$ decoding cognate and wobble codons, AAA and AAG, respectively. **(a)**The ms^{2}t^{6}A$_{37}$ stacks strongly with A$_{38}$, making use of the *N*^{6}-threonylcarbamoyl moiety to increase area of interaction. **(b)** The ms^{2}t^{6}A$_{37}$ does not stack with U$_{36}$ (both with carbons colored **slate**), but instead forms a cross-strand stack involving its 2-methylthio modification with A1 of the codon (carbons colored **cyan**), which is hydrogen bonded to U$_{36}$ (**black** dotted lines). **(c)** The positioning of the t^6 and ms^2-groups within the structures of the hASL$^{Lys3}_{UUU}$-mcm^{5}s^{2}U$_{34}$;ms^{2}t^{6}A$_{37}$;ψ$_{39}$ (carbons colored **slate**) and the ASL$^{Lys3}_{UUU}$-t^{6}A$_{37}$ (carbons colored **grey**). The ribosomal crystal structures bound to the AAA codon are superimposed using the backbones as a register. The modified A$_{37}$ residues including the t^6-moieties (carbons colored **pink**) superimpose with the ms^2-moiety clearly directed away from the ASL.

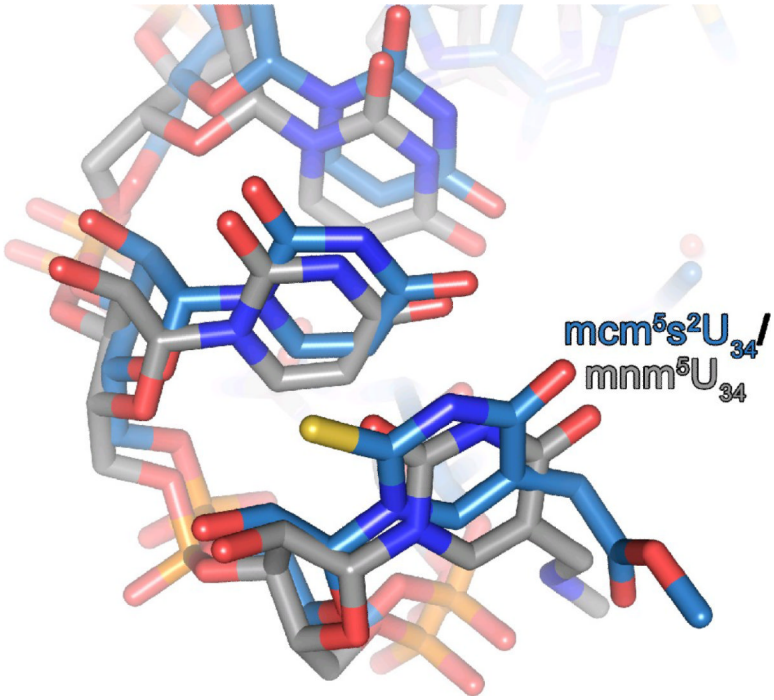

Figure 6.

The anticodon structure of hASL$^{Lys3}_{UUU}$-mcm^{5}s^{2}U$_{34}$;ms^{2}t^{6}A$_{37}$;ψ$_{39}$ in the ribosomal A-site compared to that of the ASL$^{Lys3}_{UUU}$-mnm^{5}U$_{34}$;t^{6}A$_{37}$. The crystallographic structures of the hASL$^{Lys3}_{UUU}$-mcm^{5}s^{2}U$_{34}$;ms^{2}t^{6}A$_{37}$;ψ$_{39}$ (**blue**) and that of the ASL$^{Lys3}_{UUU}$-mnm^{5}U$_{34}$;t^{6}A$_{37}$ (**grey**)in the ribosomal A-site are superimposed to reveal differences in the anticodon conformations. The s^2-moiety of mcm^{5}s^{2}U$_{34}$ stacks on the nucleobase of U$_{35}$. The positioning of the methyl groups of the mcm^5 and mnm^5 do not correspond due to the weak electron density at the extremities of the side chains.

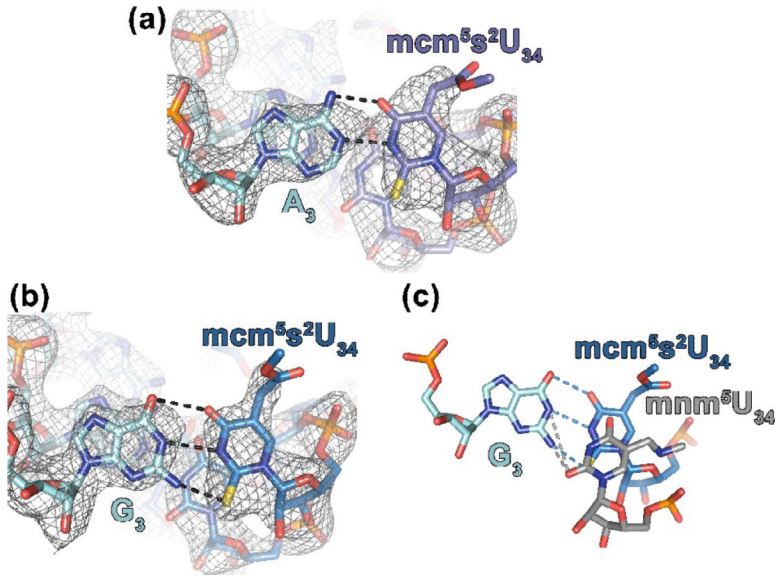

Figure 7.

Cognate and wobble codon recognition by hASL$^{Lys3}_{UUU}$ employs keto-enoltautomerism. **(a)** hASL$^{Lys3}_{UUU}$-mcm^{5}s^{2}U$_{34}$;ms^{2}t^{6}A$_{37}$;ψ$_{39}$ bound to AAA in the ribosomal A-site. The mcm^{5}s^{2}U$_{34}$ (carbons**slate**) base pairs with A$_3$ of the codon in the canonical Watson-Crick geometry. **(b)**The hASL$^{Lys3}_{UUU}$-mcm^{5}s^{2}U$_{34}$;ms^{2}t^{6}A$_{37}$;ψ$_{39}$ (carbons **blue**) recognition of the wobble codon AAG. When paired with G3 (**cyan**), the Watson-Crick geometry of a C•G base pair is maintained for this mcm^{5}s^{2}U$_{34}$•G3 pair. This requiresthe tautomericenol form of mcm^{5}s^{2}U$_{34}$. The electron density of the 2f$_o$-f$_c$ maps, shown at 1.5σ, clearly indicates the positioning of the modifications.**(c)** Comparison of the hASL$^{Lys3}_{UUU}$-mcm^{5}s^{2}U$_{34}$;ms^{2}t^{6}A$_{37}$;ψ$_{39}$ and ASL$^{Lys}_{UUU}$-mnm^{5}U$_{34}$;^{6}A$_{37}$ recognitions of the wobble codon AAG. The mnm^{5}U$_{34}$ (carbons **grey**) in the mnm^{5}U$_{34}$•G3 base pair[25] is superimposed on the mcm^{5}s^{2}U$_{34}$ (carbons **blue**) of the mcm^{5}s^{2}U$_{34}$•G3 (**cyan**) using the G3 as a reference. The mcm^5-moiety alters the electronic structure of the ring producing a shift toward the enol tautomer. The positioning of the mcm^{5}s^{2}U$_{34}$ can be attributed to the stereochemical restrictions imposed by the larger sulfur atom at position 2 of the uridine as compared to that of the oxygen. For lack of sufficient electron density to accurately place the extremes of the 5-position moieties, the differing geometries of the methoxy- of mcm^{5}s^{2}U$_{34}$ and the aminomethyl of mnm^{5}U$_{34}$ are not considered significant.

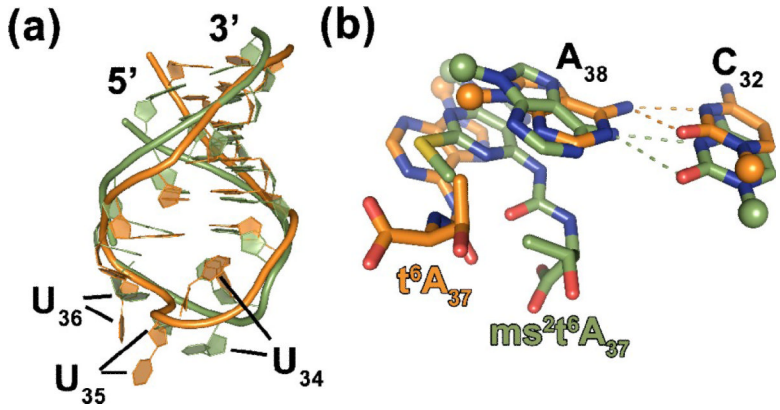

Figure 8.

Comparison of the NMR-derived solution structures.**(a)**A comparison of the NMR structure of the singly modified hASL$^{Lys3}_{UUU}$-t_6A_{37} (**orange**)[53]to that of the doubly modified hASL$^{Lys3}_{UUU}$-$mcm^5s^2U_{34}$;$ms^2t^6A_{37}$ (**green**) shows the high degree of deviation in the backbone in the anticodon loop. **(b)** A zoomed view of the potential bifurcated hydrogen bonding between C_{32} and A_{38} indicates that the prospective of stacking with the heterotricyclic ring system of A_{37} competes with the cross-loop interaction, widening the distance between these nucleosides.

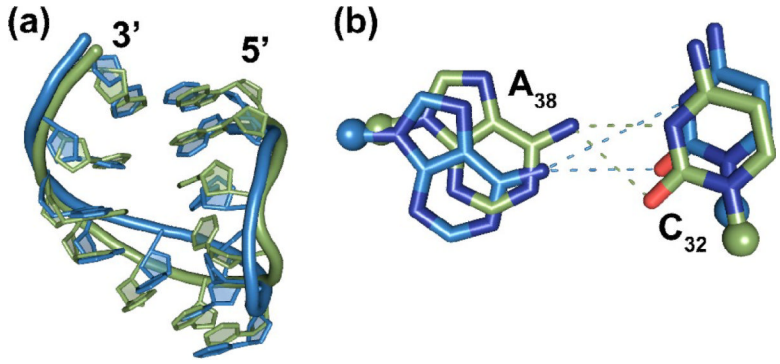

Figure 9.

Comparison of the crystal structure bound to the A-site AAG codon to the NMR-derived solution structure of the hASL$^{Lys3}_{UUU}$-mcm^{5}s^{2}U$_{34}$,ms^{2}t^{6}A$_{37}$. **(a)** The NMR-derived solution structure (**green**) has an rmsd from the AAA bound crystal structure of 1.91 Å (not shown) and the AAG bound crystal structure of 1.81 Å (**blue**). **(b)** The C$_{32}$•A$_{38}$ cross-loop interaction shows the difference between the NMR and crystal structures that is induced by the weakened base pairing between the stem residues A$_{31}$ and ψ$_{39}$.

Table 1

Thermodynamic properties derived from UV-monitored thermal denaturation and renaturation.

	hASL^{Lys3}-Unmodified	hASL^{Lys3}-mcm^{5}s^{2}U$_{34}$;ms^{2}t^{6}A$_{37}$	hASL^{Lys3}-mcm^{5}s^{2}U$_{34}$;ms^{2}t^{6}A$_{37}$;Ψ$_{39}$
ΔH (kcal/mol)	−45.66 ± 4.32	−41.69 ± 1.76	−46.73 ± 7.74
ΔS (cal/K*mol)	−139.90 ± 13.30	−127.97 ± 5.46	−143.10 ± 23.66
ΔG$_{37}$ (kcal/mol, 37 °C)	−2.76 ± 0.28	−2.00 ± 0.15	−2.34 ± 0.42
T$_m$ (°C)	56.82 ± 1.37	52.67 ± 1.12	53.37 ± 1.16
Hyperchromicity (%)	13.3 ± 0.80	11.0 ± 0.80	13.9 ± 1.50